

Journal Pre-proof

Syntheses of novel 2-oxo-1,2-dihydroquinoline derivatives: Molecular and crystal structures, spectroscopic characterizations, Hirshfeld surface analyses, molecular docking studies and density functional theory calculations

Yassir Filali Baba, Halil Gökce, Youssef Kandri Rodi, Sonia Hayani, Fouad Ouazzani Chahdi, Abdellatif Boukir, Jerry P. Jasinski, Manpreet Kaur, Tuncer Hökelek, Nada Kheira Sebbar, El Mokhtar Essassi

PII: S0022-2860(20)30786-9

DOI: <https://doi.org/10.1016/j.molstruc.2020.128461>

Reference: MOLSTR 128461

To appear in: *Journal of Molecular Structure*

Received Date: 5 January 2020

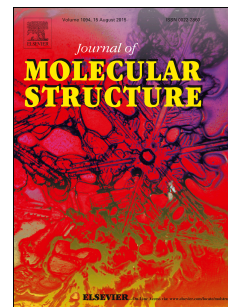
Revised Date: 12 May 2020

Accepted Date: 14 May 2020

Please cite this article as: Y.F. Baba, H. Gökce, Y.K. Rodi, S. Hayani, F.O. Chahdi, A. Boukir, J.P. Jasinski, M. Kaur, T. Hökelek, N.K. Sebbar, E.M. Essassi, Syntheses of novel 2-oxo-1,2-dihydroquinoline derivatives: Molecular and crystal structures, spectroscopic characterizations, Hirshfeld surface analyses, molecular docking studies and density functional theory calculations, *Journal of Molecular Structure* (2020), doi: <https://doi.org/10.1016/j.molstruc.2020.128461>.

This is a PDF file of an article that has undergone enhancements after acceptance, such as the addition of a cover page and metadata, and formatting for readability, but it is not yet the definitive version of record. This version will undergo additional copyediting, typesetting and review before it is published in its final form, but we are providing this version to give early visibility of the article. Please note that, during the production process, errors may be discovered which could affect the content, and all legal disclaimers that apply to the journal pertain.

© 2020 Published by Elsevier B.V.



Syntheses of novel 2-oxo-1,2-dihydroquinoline derivatives: molecular and crystal structures, spectroscopic characterizations, Hirshfeld surface analyses, molecular docking studies and Density Functional Theory calculations.

Yassir Filali Baba^a, Halil Gökce^b, Youssef Kandri Rodi^a, Sonia Hayani^a, Fouad Ouazzani Chahdi^a, Abdellatif Boukir^c, Jerry P. Jasinski^d, Manpreet Kaur^d, Tuncer Hökelek^e, Nada Kheira Sebbar^{f,g*}, El Mokhtar Essassi^f

^aLaboratory of Applied Organic Chemistry, Faculty of Science and Techniques, Sidi Mohamed Ben Abdellah University, B.P. 2202, Routed 'Imouzzar, Fez 30050, Morocco;

^bGiresun University, Vocational High School of Health Services, Department of Medical Services and Techniques, 28100 Giresun, Turkey;

^cLaboratory of Biotechnology Microbien and Molecules Bioactives LB2MB, Faculty of Science and Techniques, Sidi Mohamed Ben Abdellah University, B.P. 2202, Route 'Imouzzar, Fez 30050, Morocco;

^dDepartment of Chemistry, Keene State College, 229 Main Street, Keene, NH 03435-2001, USA;

^eDepartment of Physics, Hacettepe University, 06800 Beytepe, Ankara, Turkey;

^fLaboratoire de Chimie Appliquée et Environnement, Equipe de Chimie Bioorganique Appliquée, Faculté des sciences, Université Ibn Zohr, Agadir, Morocco;

^gLaboratoire de Chimie Organique Hétérocyclique, Centre de Recherche des Sciences des Médicaments, Pôle de Compétences Pharmacochimie, Mohammed V University in Rabat, Faculté des Sciences, Av. Ibn Battouta, BP 1014 Rabat, Morocco.

Abstract

Sixteen new quinoline derivatives (**3–18**) have been synthesized through cyclocondensation, nucleophilic substitution and alkylation reactions. All the obtained compounds have been characterized using ¹H-, ¹³C- and ¹⁹F-NMR spectroscopic measurements. The molecular and crystal structures of four of these compounds (**10**, **11**, **15** and **18**) have also been further examined by single crystal X-ray crystallography. The predicted spectral data were also obtained and compared to the experimental results using density functional theory (DFT). in order to understand the non-bonding intermolecular interactions in solid phase crystal packing. The closest contacts between active atoms of the four studied molecules were identified through both 2D and 3D Hirshfeld surface analyses. The different structures of the four compounds are optimized and their both energies highest occupied molecular orbitals (HOMO) and lowest unoccupied molecular orbitals (LUMO), as well as their clouds are evaluated. The obtained experimental results are correlated to the calculated ones and showed great compatibility. Finally, molecular docking studies are performed to investigate the binding patterns of the title compounds with the Protein Data Bank (PDB: 1M17) inhibitor targets and showed good insights on the possible interactions using the Auto-Dock Vina program.

Keywords: Quinolines, NMR Characterization, X-ray Crystallography, Molecular docking, Hirshfeld surface analysis, DFT calculations.

Corresponding authors:

Dr. Nada Kheira Sebbar

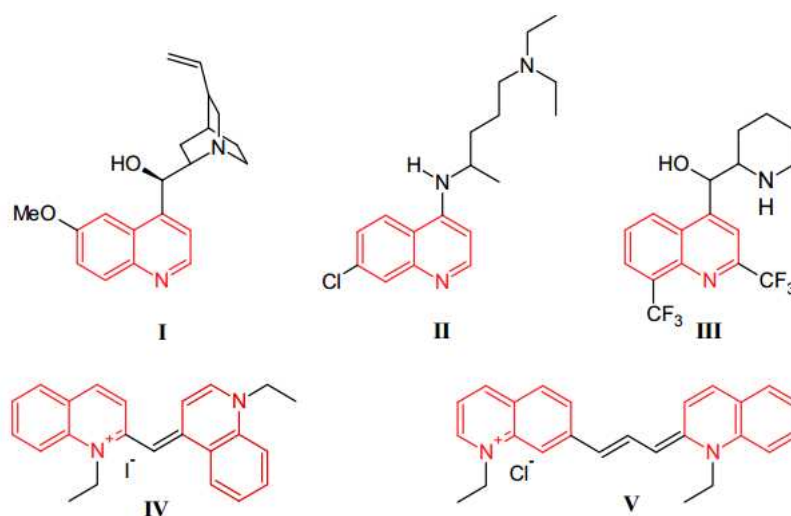
Tel:+212615011615;E-mail:snounousebbar@gmail.com

1. Introduction

Heterocyclic compounds have paved the way for interesting achievements in the fight against many life-threatening diseases [1]. These compounds offer a high degree of structural diversity conferring a broad spectrum to the therapeutic field. Therefore, it is not surprising that the development of new synthesis methodologies of new biologically active heterocyclic compounds constitutes a very important goal for synthetic organic chemists [2]. Quinolines and their derivatives have contributed substantially to the regression of microbial diseases. The development of quinolone-based antibiotics began in 1962 with the discovery of nalidixic acid, which was used to treat urinary tract infections [3]. Quinoline derivatives are a classical division of organic chemistry and many of these molecules have shown remarkable biological properties, including exceptional activities, such as, antimalarial [4], antibacterial [5-6], antifungal [7], anticancer [8-9] and anti-inflammatory [10-11] effects. Some of these compounds are endowed with other various activities, such as antituberculosis [12], analgesic [13], cardiovascular [14], antibiotic [15], antihypertensive [16], tyrosine kinase (PDGF-RTK) inhibition [17] and anti-HIV [18-19]. Additionally, the quinoline ring plays an important role in the development of new antitumoral agents, as their derivatives have shown excellent results through different mechanisms of action. They are growth inhibitors by cell cycle arrest, apoptosis agents, angiogenesis inhibitors, disruption of cell migration, and modulation of nuclear receptor responsiveness [20-21]. Furthermore, the quinine **I** (Scheme 1) was the first and most widely used as antimalarial agent due especially to the presence of the quinoline scaffold, followed by closely related derivatives, chloroquine **II** (Scheme 1) and mefloquine **III** (Scheme 1) [22]. Several promising anti-inflammatory and antitumor therapeutic agents are also built on quinoline structure. Alternatively, quinoline derivatives provide a framework for industrial use, including organic light-emitting diodes (OLEDs) and photovoltaic cells, as well as solvents for terpenes and resins [23]. In addition, quinoline-based dyes such as ethyl red iodide **IV** (Scheme 1) and pinacyanol **V** (Scheme 1) have been used as a pigment for photographic plates since the nineteenth century according to their heterocyclic aromatic chromophore and basic characteristics [24].

Due to its presence and importance as pharmacophore in a wide range of natural and synthesized products, the development of new quinoline-based structures requires a great effort of synthesis methodology and architectural design. This is a quintessential aspect of our research. The objective of this work is to prepare and characterize new 2-oxo-1,2-dihydroquinoline carboxamide derivatives (3-18) in multi-step methodology. The starting

material containing quinoline moiety, is achieved by a cyclocondensation reaction involving isatin and malonic acid in refluxing acetic acid in the presence of sodium acetate. The compound 1 obtained reacts with an excess of thionyl chloride, leading to quinoline-4-carboxylic acid chloride 2 which in turn reacts with various substituted anilines, 2,4-difluoroaniline; 3-chloro-4-fluoroaniline and 3-trifluoromethyl-aniline, to afford the new quinolines 3-6. Furthermore, the alkylation reactions of the four latter compounds with three different alkyl halides, such as, ethyl iodide, propargyl bromide and ethyl bromoacetate, are carried out in phase transfer catalysis conditions allowing the formation of the new dialkylated compounds 7-18, whose structures have been elucidated by spectral data (Nuclear Magnetic Resonance ^1H , ^{13}C and ^{19}F). The structures of compounds 10, 11, 15 and 18 were confirmed by single crystal X-ray diffraction. The structures assigned were also confirmed by predicting the corresponding spectroscopic data and Z-matrix coordinates using DFT theoretical calculations at the B3LYP/6-311G (d,p) level of theory and molecular docking studies from the Protein Data Bank (PDB: 1M17) on an inhibitor were carried out using Auto-Dock Vina program. Compounds 10, 11, 15 and 18 were further studied by Hirshfeld surface analyses, molecular docking studies, and DFT calculations.



Scheme 1. Chemical structures of quinine (I), chloroquine (II), mefloquine (III), ethyl red iodide (IV) and pinacyanol (V).

2. Material and methods

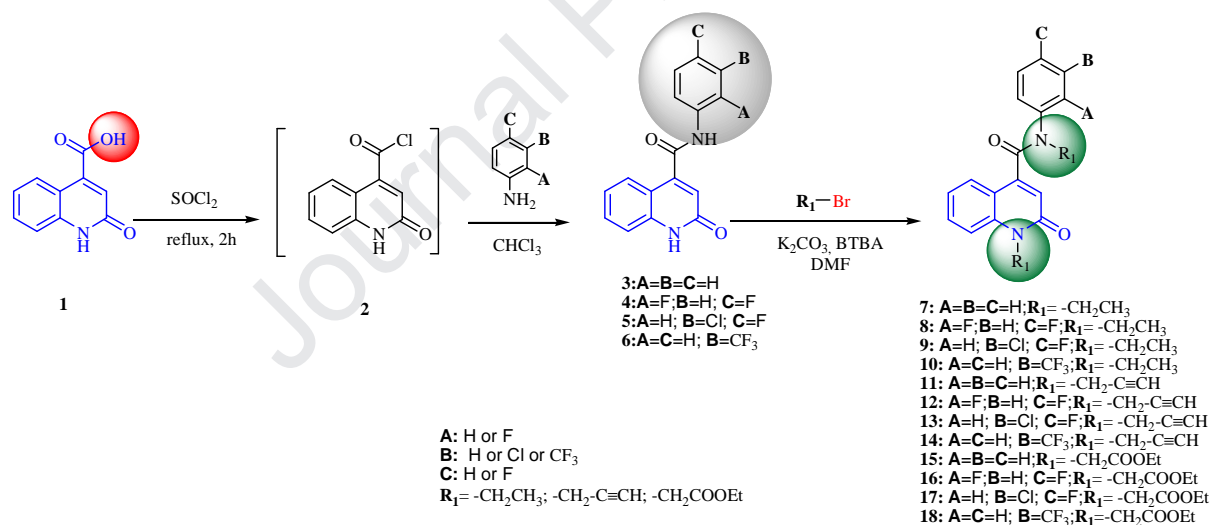
2.1. Spectral data measurements

The spectroscopic characterizations of the synthesized compounds (3-18) were achieved by recording their NMR spectra: ^1H NMR (300 MHz), ^{13}C NMR (75 MHz), ^{19}F NMR (282 MHz), respectively, which were measured on a Bruker Advance DPX 300 instrument, using CDCl_3 and DMSO-d_6 as solvents. The chemical shifts (δ) were expressed in ppm and the coupling

constants (J) in Hertz (Hz) and their multiplicities were expressed as: m = multiplet, q = quartet, t = triplet, dd = double doublet, d = doublet, and s = singlet, down field from TMS [tetramethylsilane, Si(CH₃)₄], which has been assigned to a chemical shift of zero, and used as an internal reference. Thin layer chromatography (TLC) and column chromatography were carried out on silica plates (Merck 60 F254) and silica gel (Merck 60, 230-400 mesh), respectively. Melting points of compounds (3-18) were measured in open capillaries and were uncorrected.

2.2. Preparation of compounds (7-18) by alkylation reaction under PTC conditions

Derivative **1** reacts with an excess of thionyl chloride (SOCl₂), forming intermediate **2** which is used later for an acylation reaction by a variety of aniline derivatives (aniline, 2,4-difluoroaniline, 3-chloro-4-fluoroaniline or 3-trifluoromethyl-aniline). The reaction leads to new quinoline derivatives (**3-6**) with excellent yields. Prominently, the alkylation of 2-oxo-N-phenyl-1,2-dihydroquinoline-4-carboxamide derivatives (**3-6**) with ethyl iodide, propargyl bromide and ethyl bromoacetate prompts the formation of the dialkylated compounds (**7-18**) with good yields (Scheme 2).



Scheme 2. Syntheses of 2-oxo-1,2-dihydroquinoline carboxamide derivatives (3-6) and their N-alkylated derivatives (7-18).

2.3. Synthesis of compound 1: 2-oxo-1,2-dihydroquinoline-4-carboxylic acid:

To a solution of 10 mmol of isatin and 10 mmol of malonic acid in 30 ml of acetic acid was added 1 mmol of sodium acetate. The mixture was refluxed for 24 h. After cooling, 100 ml of ice-water were added. The precipitate obtained was washed several times with ethanol [25].

Yield (%) = 90; mp = 553 K; ¹H NMR (300 MHz, CDCl₃): 6.86 (s, 1H, CH); 7.2-8.16 (m, 4H, CH_{arom}); 12.17 (s, 1H, NH); 13.9 (s, 1H, OH). ¹³C NMR (75 MHz, CDCl₃): 167.2 (COOH),

163.0 (C=O), 141.7-139.8 (Cq-Cq), 131.3 (CH_{arom}), 126.5 (CH_{arom}), 123.8 (CH), 122.6 (Cq), 116.2 (CH_{arom}).

*** General procedure: syntheses of the compounds (3-6)**

✓ *Step 1 : acyl chloride preparation*

To 10 mmol of the product **1**, 10-15 ml of thionyl chloride (SOCl₂) was added, the mixture was then refluxed for 2 h. The excess of thionyl chloride was evaporated under reduced pressure, and then the intermediate acyl chloride **2** was obtained, and used immediately for the next step without any purification.

✓ *Step 2 : action of aniline derivatives*

To the acyl chloride **2** in 10 ml of chloroform, were added at 0°C 1.5 eq of an aniline derivative (aniline, 2,4-difluoroaniline, 3-chloro-4-fluoroaniline or 3-trifluoromethyl-aniline). The reaction mixture was left at room temperature for 2 h. Then, the residue obtained was recrystallized from the mixture of solvents (DMSO / H₂O), leading to the formation of the new carboxamide compounds (**3-6**).

2-oxo-N-phenyl-1,2-dihydroquinoline-4-carboxamide: 3

Yield (%) = 92; mp > 623 K; ¹H NMR (300 MHz, DMSO-d₆): 6.93 (s, 1H, CH_{arom}), 7.15 (t, 1H, ³J_{H-H} = 7.2 Hz, CH_{arom}), 7.22 (t, 1H, ³J_{H-H} = 7.2 Hz, CH_{arom}), 7.38 (m, 3H, CH_{arom}), 7.56 (td, 1H, ³J_{H-H} = 7.2 Hz, ⁴J_{H-H} = 1.1 Hz, CH_{arom}), 7.73 (t, 1H, ³J_{H-H} = 7.7 Hz, CH_{arom}), 10.74 (s, 1H, NH), 12.02 (s, 1H, NH). ¹³C NMR (75 MHz, DMSO-d₆): 164.77 (C=O), 161.82 (C=O), 146.48 (Cq), 139.68-138.93 (Cq-Cq), 131.49 (CH_{arom}), 129.31 (2 CH_{arom}), 126.17 (CH_{arom}), 124.76 (CH_{arom}), 122.79 (CH_{arom}), 120.48 (2 CH_{arom}), 120.33 (CH_{arom}), 116.47 (Cq), 116.24 (CH_{arom}).

N- (2,4-difluorophenyl) -2-oxo-1,2-dihydroquinoline-4-carboxamide: 4

Yield (%) = 98 %; mp > 623 K; ¹H NMR (300 MHz, DMSO-d₆): 6.72 (s, 1H, CH_{arom}), 7.13-7.26 (m, 2H, CH_{arom}), 7.36-7.44 (m, 2H, CH_{arom}), 7.54-7.6 (m, 1H, CH_{arom}), 7.74-7.82 (m, 1H, CH_{arom}), 10.57 (s, 1H, NH), 12.02 (s, 1H, NH). ¹³C NMR (75 MHz, DMSO-d₆): 165.22 (C=O), 161.61 (C=O), 160.23 (dd, Cq, ¹J_{C-F} = 243.75 Hz, ³J_{C-F} = 11.25 Hz), 156 (dd, Cq, ¹J_{C-F} = 248.25 Hz, ³J_{C-F} = 12.75 Hz), 145.88 (Cq), 139.75 (Cq), 131.47 (CH_{arom}), 128.3 (dd, CH_{arom}, ⁴J = 9.9 Hz, ⁴J = 2.85 Hz), 126.13 (CH_{arom}), 122.69 (CH_{arom}), 121.85 (dd, CH_{arom}, ²J = 12.67 Hz, ⁴J = 4.5 Hz), 120.8 (CH_{arom}), 116.45 (Cq), 116.22 (CH_{arom}), 111.8 (dd, CH_{arom}, ²J = 22.5 Hz, ⁴J = 3.75 Hz), 104.97 (dd, CH_{arom}, ²J = 24 Hz, ²J = 24 Hz). ¹⁹F NMR (282 MHz, DMSO-d₆): δ = -112.69 (d, 1F, ³J_{C-F} = 6,2 Hz), δ = -116.70 ppm (d, 1F, ³J_{C-F} = 6,2 Hz).

N- (3-chloro-4-fluorophenyl) -2-oxo-1,2-dihydroquinoline-4-carboxamide: 5

Yield (%) = 93 %; mp > 623 K; ^1H NMR (300 MHz, DMSO- d_6): 6.75 (s, 1H, CH_{arom}), 7.24 (t, 3H, $^3\text{J}_{\text{H-H}} = 7.2$ Hz, CH_{arom}), 7.37-7.67 (m, 4H, CH_{arom}), 7.74 (d, 1H, $^3\text{J}_{\text{H-H}} = 7.8$ Hz, CH_{arom}), 8.08 (dd, 1H, $^3\text{J}_{\text{H-H}} = 6.9$ Hz, $^4\text{J}_{\text{H-H}} = 2.4$ Hz, CH_{arom}), 10.93 (s, 1H, NH); 12.04 (s, 1H, NH). ^{13}C NMR (75 MHz, DMSO- d_6): 164.89 (C=O), 161.63 (C=O), 154.15 (d, Cq, $^1\text{J}_{\text{C-F}} = 242.25$ Hz), 145.88-139.77 (Cq-Cq), 136.22 (d, Cq, $^4\text{J}_{\text{C-F}} = 3.75$ Hz), 131.53 (CH_{arom}), 126.22 (CH_{arom}), 122.75 (CH_{arom}), 122.03 (CH_{arom}), 120.95 (d, CH_{arom} , $^3\text{J}_{\text{C-F}} = 6.75$ Hz), 120.84 (d, CH_{arom} , $^3\text{J}_{\text{C-F}} = 7.5$ Hz), 119.7 (d, Cq, $^2\text{J}_{\text{C-F}} = 18$ Hz), 117.55 (d, CH_{arom} , $^2\text{J}_{\text{C-F}} = 21.75$ Hz), 116.27 (Cq), 116.23 (CH_{arom}). ^{19}F NMR (282 MHz, DMSO- d_6): $\delta = -121.47$ ppm.

2-oxo-N- (3 - (trifluoromethyl) phenyl) -1,2-dihydroquinoline-4-carboxamide: 6

Yield (%) = 91 %; mp > 623 K; ^1H NMR (300 MHz, DMSO- d_6): 6.79 (s, 1H, CH_{arom}), 7.22 (td, 1H, $^3\text{J}_{\text{H-H}} = 6.9$ Hz, $^4\text{J}_{\text{H-H}} = 0.9$ Hz, CH_{arom}), 7.39 (d, 1H, $^3\text{J}_{\text{H-H}} = 8.1$ Hz, CH_{arom}), 7.50-7.74 (m, 2H, CH_{arom}), 7.76 (dd, 1H, $^3\text{J}_{\text{H-H}} = 8.1$ Hz, $^4\text{J}_{\text{H-H}} = 0.6$ Hz, CH_{arom}), 7.96 (d, 1H, $^3\text{J}_{\text{H-H}} = 8.1$ Hz, CH_{arom}), 8.27 (s, 1H, CH_{arom}), 11.08 (s, 1H, NH), 12.08 (s, 1H, NH). ^{13}C NMR (75 MHz, DMSO- d_6): 165.19 (C=O), 161.66 (C=O), 145.87 (Cq), 139.80-139.76 (Cq-Cq), 131.53 (CH_{arom}), 130.59 (CH_{arom}), 129.97 (q, Cq, $^3\text{J}_{\text{C-F}} = 31.5$ Hz), 126.34 (Cq), 126.22 (CH_{arom}), 124.03 (CH_{arom}), 122.76 (CH_{arom}), 122.03 (CH_{arom}), 121.03 (q, CH_{arom} , $^3\text{J}_{\text{C-F}} = 4.5$ Hz), 120.85 (CH_{arom}), 116.53 (q, CH_{arom} , $^3\text{J}_{\text{C-F}} = 4.5$ Hz), 116.27 (Cq), 116.24 (CH_{arom}). ^{19}F NMR (282 MHz, DMSO- d_6): $\delta = -61.32$ ppm (3F, CF_3).

General procedure: syntheses of the compounds (7-18)Strategies for functionalization of the two amide functions*

10 mmols of each of the compounds derived from 2-oxo-1,2-dihydroquinoline-4-carboxamide (**3**, **4**, **5** and **6**) in 10 ml of DMF were mixed with 2.2 eq of (ethyl iodide, propargyl bromide or ethyl bromoacetate), 5 eq of K_2CO_3 and 0.1 eq of tetra n-butylammonium bromide (TBAB). The reaction mixture was stirred at room temperature in DMF for 6 h. After removal of the salts by filtration, the DMF was evaporated under reduced pressure, and the resulting residues were dissolved in dichloromethane. The organic phase was dried over Na_2SO_4 and then concentrated under vacuum. The pure compound was separated on column liquid chromatography, using a mixture of hexane / ethyl acetate (3/1) as eluent, allowing to the preparation of the new and various N-alkylated carboxamide compounds (**7-18**).

N-ethyl, N-phenyl- (1-ethyl-2-oxo-1,2-dihydroquinoline-4)-carboxamide: 7

Yield (%) = 76 %; mp > 414,15 K; ^1H NMR (300 MHz, CDCl_3): 1.25 (t, 3H, $^3\text{J}_{\text{H-H}} = 7.2$ Hz, CH_3), 1.31 (t, 3H, $^3\text{J}_{\text{H-H}} = 7.2$ Hz, CH_3), 4.05 (q, 2H, $^3\text{J}_{\text{H-H}} = 7.2$ Hz, CH_2), 4.23 (q, 2H, $^3\text{J}_{\text{H-H}} = 7.2$ Hz, CH_2), 6.37 (s, 1H, CH_{arom}); 7.04-7.07 (m, 2H, CH_{arom}); 7.15-7.19 (m, 3H, CH_{arom}),

7.26-7.33(m, 2H, CH_{arom}), 7.56 (m, 1H, CH_{arom}), 7.8(m, 1H, CH_{arom}).¹³C NMR (75 MHz, CDCl₃): 166.44 (C=O), 160.67 (C=O), 145.22 (Cq), 141.15-139.05 (Cq-Cq), 130.92 (CH_{arom}), 129.45 (2CH_{arom}), 127.99 (CH_{arom}), 127.63 (2CH_{arom}), 127.01 (CH_{arom}), 122.21 (CH_{arom}), 119.93 (CH_{arom}), 118.44 (Cq), 114.40 (CH_{arom}), 44.46 (CH₂), 37.19 (CH₂), 13.06 (CH₃), 12.57 (CH₃).

N-ethyl, N-(2,4-difluorophenyl)- (1-ethyl-2-oxo-1,2-dihydroquinoline-4)-carboxamide: 8

Yield (%) = 65 %; mp > 416,15 K; ¹H NMR (300 MHz, CDCl₃) : 1.26 (t, 3H, ³J_{H-H} = 7.2 Hz, CH₃), 1.33 (t, 3H, ³J_{H-H} = 7.2 Hz, CH₃), 4.09 (q, 2H, ³J_{H-H} = 7.2 Hz, CH₂), 4.24 (q, 2H, ³J_{H-H} = 7.2 Hz, CH₂), 6.47 (s, 1H, CH_{arom}), 6.68-6.80 (m, 2H, CH_{arom}), 7.05 (m, 1H, CH_{arom}), 7.23-7.74 (m, 5H, CH_{arom}).¹³C NMR (75 MHz, CDCl₃): 166.92 (C=O), 162.24 (dd, Cq, ¹J_{C-F} = 231 Hz, ³J_{C-F} = 12 Hz), 160.53 (C=O), 158.30 (dd, Cq, ¹J_{C-F} = 251.25 Hz, ³J_{C-F} = 12 Hz), 144.67 (Cq), 139.15 (Cq), 131.15 (CH_{arom}), 130.9 (dd, CH_{arom}, ⁴J = 9.75 Hz, ⁴J = 2.85 Hz), 126.84 (CH_{arom}), 125.24 (dd, Cq, ⁴J = 11.77 Hz, ⁴J = 4.5 Hz), 122.19 (CH_{arom}), 119.09 (m, CH_{arom}), 118.00 (CH_{arom}), 117,79 (Cq), 114,40 (CH_{arom}), 111.98 (dd, CH_{arom}, ²J = 22.5 Hz, ⁴J = 4.5 Hz), 105.35 (dd, CH_{arom}, ²J = 25.5 Hz), 43.91 (CH₂), 37.32 (CH₂), 12.70 (CH₃), 12.56 (CH₃). ¹⁹F NMR (282 MHz, CDCl₃): δ = -112.69 (d, 1F, ³J_{C-F} = 6,2 Hz), δ = -116.70 ppm (d, 1F, ³J_{C-F} = 6,2 Hz).

N-ethyl, N-(3-chloro-4-fluorophenyl)- (1-ethyl-2-oxo-1,2-dihydroquinoline-4)-carboxamide: 9

Yield (%) = 80 %; mp > 419,15 K; ¹H NMR (300 MHz, CDCl₃) : 1.28 (t, 3H, ³J_{H-H} = 7.2 Hz, CH₃), 1.30 (t, 3H, ³J_{H-H} = 7.2 Hz, CH₃), 4.02 (q, 2H, ³J_{H-H} = 7.2 Hz, CH₂), 4.26 (q, 2H, ³J_{H-H} = 7.2 Hz, CH₂), 6.38 (s, 1H, CH_{arom}), 6.94 (dd, 2H, ³J_{H-H} = 6.3 Hz, ⁴J_{H-H} = 1.2 Hz, CH_{arom}), 7.16 (m, 1H, CH_{arom}), 7.26-7.37 (m, 2H, CH_{arom}), 7.56-7.72 (m, 2H, CH_{arom}).¹³C NMR (75 MHz, CDCl₃): 166.29 (C=O), 160.50 (C=O), 159.02 (Cq), 157.35 (d, Cq, ¹J_{C-F} = 250.5 Hz), 144.77-139.13 (Cq-Cq), 137.85 (Cq), 131.25 (CH_{arom}), 129.72 (CH_{arom}), 127.7 (d, CH_{arom}, ³J_{C-F} = 7.5 Hz), 126.63 (CH_{arom}), 122.35 (CH_{arom}), 121.8 (d, Cq, ²J_{C-F} = 18.9 Hz), 119.89 (CH_{arom}), 118.06 (Cq), 117.20 (d, CH_{arom}, ³J_{C-F} = 7.5 Hz), 117.55 (d, CH_{arom}, ²J_{C-F} = 22.12 Hz), 114.61 (CH_{arom}), 44.62 (CH₂), 37.34 (CH₂), 13.00 (CH₃), 12.57 (CH₃). ¹⁹F NMR (282 MHz, CDCl₃) : δ = -114.64 ppm.

N-ethyl, N-(3-trifluoromethylphenyl)- (1-ethyl-2-oxo-1,2-dihydroquinoline-4)-carboxamide: 10

Yield (%) = 63 %; mp > 422,15 K; ¹H NMR (300 MHz, CDCl₃) : 1.25 (t, 3H, ³J_{H-H} = 7.2 Hz, CH₃), 1.33 (t, 3H, ³J_{H-H} = 7.2 Hz, CH₃), 4.09 (q, 2H, ³J_{H-H} = 7.2 Hz, CH₂), 4.24 (q, 2H, ³J_{H-H} = 7.2 Hz, CH₂), 6.35 (s, 1H, CH_{arom}), 7.26-7.43 (m, 5H, CH_{arom}), 7.56-7,77 (m, 3H, CH_{arom}).¹³C

NMR (75 MHz, CDCl₃): 166.43 (C=O), 163.05 (C=O), 145.87 (Cq), 139.80-139.22 (Cq-Cq), 131.28 (CH_{arom}), 130.79 (CH_{arom}), 130.14 (CH_{arom}), 129.45 (q, Cq, ³J_{C-F} = 31.5 Hz), 126.82 (Cq), 126.65 (CH_{arom}), 124.70 (q, CH_{arom}, ³J_{C-F} = 3.75 Hz), 124.17 (q, CH_{arom}, ³J_{C-F} = 3.75 Hz), 122.40 (CH_{arom}), 119.21 (CH_{arom}), 116.27 (Cq), 114.57 (CH_{arom}), 44.50 (CH₂), 37.23 (CH₂), 13.04 (CH₃), 12.49 (CH₃). ¹⁹F NMR (282 MHz, CDCl₃): δ = -61.32 ppm (3F, CF₃).

N- (prop-2-yn-1-yl), N-phenyl- (1-prop-2-yn-1-yl -2-oxo-1,2-dihydroquinoline-4)-carboxamide: 11

Yield (%) = 75 %; mp > 424,15 K; ¹H NMR (300 MHz, CDCl₃): 2.21 (t, 1H, ⁴J_{H-H} = 2.4 Hz, ≡CH), 2.36 (t, 1H, ⁴J_{H-H} = 2.4 Hz, ≡CH), 4.74 (d, 2H, ⁴J_{H-H} = 2.4 Hz, CH₂), 4.97 (d, 2H, ⁴J_{H-H} = 2.4 Hz, CH₂), 6.42 (s, 1H, CH_{arom}), 7.18-7.22 (m, 5H, CH_{arom}), 7.33 (td, 1H, ³J_{H-H} = 8.1 Hz, ⁴J_{H-H} = 0.9 Hz, CH_{arom}), 7.46 (d, 1H, ³J_{H-H} = 8.4 Hz, CH_{arom}), 7.6 (td, 1H, ³J_{H-H} = 7.2 Hz, ⁴J_{H-H} = 1.5 Hz, CH_{arom}), 7.81 (dd, 1H, ³J_{H-H} = 8.4 Hz, ⁴J_{H-H} = 1.2 Hz, CH_{arom}).

¹³C NMR (75 MHz, CDCl₃): 166.26 (C=O), 160.06 (C=O), 145.09 (Cq), 140.62-138.75 (Cq-Cq), 131.28 (CH_{arom}), 129.57 (2 CH_{arom}), 128.61 (CH_{arom}), 127.45 (2 CH_{arom}), 126.91 (CH_{arom}), 122.95 (CH_{arom}), 119.80 (CH_{arom}), 118.25 (Cq), 115.04 (CH_{arom}), 78.24 (C≡), 77.51 (C≡), 72.89 (≡CH), 72.60 (≡CH), 38.88 (CH₂), 31.63 (CH₂).

N- (prop-2-yn-1-yl), N-(2,4-difluorophenyl)- (1-prop-2-yn-1-yl -2-oxo-1,2-dihydroquinoline-4)-carboxamide: 12

Yield (%) = 73 %; mp > 416,15 K; ¹H NMR (300 MHz, CDCl₃): 2.22 (t, 3H, ⁴J_{H-H} = 2.4 Hz, ≡CH), 2.32 (t, 3H, ⁴J_{H-H} = 2.4 Hz, ≡CH), 4.28 (d, 2H, ⁴J_{H-H} = 2.4 Hz, CH₂), 5.00 (d, 2H, ⁴J_{H-H} = 2.4 Hz, CH₂), 6.52 (s, 1H, CH_{arom}), 6.68-7.76 (m, 8H, 8CH_{arom}). ¹³C NMR (75 MHz, CDCl₃): 164.91 (C=O), 159.94 (C=O), 160.23 (dd, Cq, ¹J_{C-F} = 243.75 Hz, ³J_{C-F} = 11.25 Hz), 156 (dd, Cq, ¹J_{C-F} = 248.25 Hz, ³J_{C-F} = 12.75 Hz), 144.53 (Cq), 138.78 (Cq), 131.49 (CH_{arom}), 128.3 (dd, CH_{arom}, ⁴J = 9.9 Hz, ⁴J = 2.85 Hz), 126.13 (CH_{arom}), 122.69 (CH_{arom}), 121.85 (dd, CH_{arom}, ²J = 12.67 Hz, ⁴J = 4.5 Hz), 119.58 (CH_{arom}), 117.68 (Cq), 115.23 (CH_{arom}), 115.07 (CH_{arom}), 112.1 (dd, CH_{arom}, ²J = 21.9 Hz, ⁴J = 3.75 Hz), 105.41 (dd, CH_{arom}, ²J = 23.7 Hz), 77.44 (C≡), 76.50 (C≡), 73.54 (≡CH), 72.70 (≡CH), 37.93 (CH₂), 31.71 (CH₂). ¹⁹F NMR (282 MHz, CDCl₃): δ = -112.69 (d, 1F, ³J = 6,2 Hz), δ = -116.70 ppm (d, 1F, ³J_{C-F} = 6,2 Hz).

N- (prop-2-yn-1-yl), N-(3-chloro-4-fluorophenyl)- (1-prop-2-yn-1-yl -2-oxo-1,2-dihydroquinoline-4)-carboxamide: 13

Yield (%) = 80 %; mp > 432,15 K; ¹H NMR (300 MHz, CDCl₃): 2.21 (t, 3H, ⁴J_{H-H} = 2.4 Hz, ≡CH); 2.39 (t, 3H, ⁴J_{H-H} = 2.4 Hz, ≡CH); 4.77 (d, 2H, ⁴J_{H-H} = 2.4 Hz, CH₂); 4.97 (d, 2H, ⁴J_{H-H} = 2.4 Hz, CH₂); 6.42 (s, 1H, CH_{arom}); 7.32-7.78 (m, 8H, CH_{arom}). ¹³C NMR (75 MHz, CDCl₃):

166.09 (C=O), 159.91 (C=O), 154.15 (d, Cq, $^1J_{C-F} = 259.5$ Hz), 144.64-138.80 (Cq-Cq), 137.01 (Cq), 131.62 (CH_{arom}), 129.82 (CH_{arom}), 127.81 (d, CH_{arom}, $^3J_{C-F} = 7.75$ Hz), 126.53 (CH_{arom}), 123.10 (CH_{arom}), 119.76 (CH_{arom}), 117.87 (Cq), 117.3 (d, CH_{arom}, $^2J_{C-F} = 51$ Hz), 115.29 (CH_{arom}), 77.,69 (C≡), 77.36 (C≡), 73.62 (≡CH), 72.78 (≡CH), 38.86 (CH₂), 31.75 (CH₂). ^{19}F NMR (282 MHz, CDCl₃) : $\delta = -114.62$ ppm.

N- (prop-2-yn-1-yl), N-(3-(trifluoromethyl)phenyl)- (1-prop-2-yn-1-yl -2-oxo-1,2-dihydroquinoline-4)-carboxamide:14

Yield (%) = 71 %; mp > 404,15 K; 1H NMR (300 MHz, CDCl₃): 2.21 (t, 3H, $^4J_{H-H} = 2.4$ Hz, ≡CH), 2.39 (t, 3H, $^4J_{H-H} = 2.4$ Hz, ≡CH), 4.77 (d, 2H, $^4J_{H-H} = 2.4$ Hz, CH₂), 4.97 (d, 2H, $^4J_{H-H} = 2.4$ Hz, CH₂); 6.42 (s, 1H, CH_{arom}); 7.32-7.78 (m, 8H, CH_{arom}). ^{13}C NMR (75 MHz, CDCl₃): 166.09 (C=O), 159.85 (C=O), 144.71 (Cq), 141.13-138.69 (Cq-Cq), 131.61 (CH_{arom}), 130.76 (CH_{arom}), 130.22 (CH_{arom}), 126.53 (CH_{arom}), 125.30 (q, CH_{arom}, $^3J_{C-F} = 4.1$ Hz), 124.22 (q, CH_{arom}, $^3J_{C-F} = 4$ Hz), 123.10 (CH_{arom}), 119.78 (CH_{arom}), 117.89 (Cq), 115.23 (CH_{arom}), 77.71 (C≡), 77.36 (C≡), 73.56 (≡CH), 72.68 (≡CH), 38.67 (CH₂), 31.56 (CH₂). ^{19}F NMR (282 MHz, CDCl₃) : $\delta = -61.32$ ppm (3F, CF₃).

N- (2-ethoxy-2-oxoethyl), N-phenyl- (1-2-ethoxy-2-oxoethyl -2-oxo-1,2-dihydroquinoline-4)-carboxamide : 15 [26]

Yield (%) = 71 % ; mp > 398,15 K; 1H NMR (300 MHz, CDCl₃): 1.18 (t, 3H, $^3J_{H-H} = 7.2$ Hz, CH₃), 1.36 (t, 3H, $^3J_{H-H} = 7.2$ Hz, CH₃), 4.16 (q, 2H, $^3J_{H-H} = 7.2$ Hz, CH₂), 4.32 (q, 2H, $^3J_{H-H} = 7.2$ Hz, CH₂), 4.65 (s, 2H, OCH₂), 4.97 (s, 2H, OCH₂), 6.49 (s, 1H, CH), 7.03-8.08 (m, 9H, CH_{arom}). ^{13}C NMR (75 MHz, CDCl₃): 168.55 (C=O), 167.72 (C=O), 167.20 (C=O), 160.71 (C=O), 145.45 (Cq), 141.67-139.29 (Cq-Cq), 131.39 (CH_{arom}), 129.58 (2CH_{arom}), 128.42 (CH_{arom}), 127.63 (CH_{arom}), 127.31 (2CH_{arom}), 123.01 (CH_{arom}), 119.47 (CH_{arom}), 118.19 (Cq), 113.81 (CH_{arom}), 61.77 (CH₂), 61.73 (CH₂), 51.53 (CH₂), 43.79 (CH₂), 14.21 (CH₃), 14.05 (CH₃).

N- (2-ethoxy-2-oxoethyl), N-(2,4-difluorophenyl)- (1-2-ethoxy-2-oxoethyl -2-oxo-1,2-dihydroquinoline-4)-carboxamide: 16

Yield (%) = 75 %; mp > 419,15 K; 1H NMR (300 MHz, CDCl₃) : 1.18 (t, 3H, $^3J_{H-H} = 7.2$ Hz, CH₃), 1.35 (t, 3H, $^3J_{H-H} = 7.2$ Hz, CH₃), 4.18 (q, 2H, $^3J_{H-H} = 7.2$ Hz, CH₂), 4.32 (q, 2H, $^3J_{H-H} = 7.2$ Hz, CH₂), 4.93 (s, 2H, OCH₂), 5.13 (s, 2H, OCH₂), 6.51 (s, 1H, CH_{arom}), 6.79-6.89 (m, 2H, CH_{arom}), 7.13 (m, 1H, CH_{arom}), 7.34-7.82 (m, 5H, CH_{arom}). ^{13}C NMR (75 MHz, CDCl₃): 167.35 (C=O), 166.79 (C=O), 165.12 (C=O), 160.93 (C=O), 160.02 (dd, Cq, $^1J_{C-F} = 243.75$ Hz, $^3J_{C-F} = 12$ Hz), 155.89 (dd, Cq, $^1J_{C-F} = 248.25$ Hz, $^3J_{C-F} = 12.75$ Hz), 145.81 (Cq), 140.05

(Cq), 131.79 (CH_{arom}), 128.3 (dd, CH_{arom}, ⁴J = 9.9 Hz, ⁴J = 2.85 Hz), 125.83 (CH_{arom}), 123.06 (CH_{arom}), 122.01 (dd, CH_{arom}, ²J = 12.75 Hz, ⁴J = 4.5 Hz), 120.76 (CH_{arom}), 116.65 (Cq), 116.42 (CH_{arom}), 112.12 (dd, CH_{arom}, ²J = 23.25 Hz, ⁴J = 4.5 Hz), 104.97 (dd, CH_{arom}, ²J = 24 Hz, ²J = 24 Hz), 61.68 (CH₂), 61.61 (CH₂), 51.50 (CH₂), 43.84 (CH₂), 14.20 (CH₃), 14.01 (CH₃). ¹⁹F NMR (282 MHz, CDCl₃): δ = -112.65 (d, 1F, ³J_{C-F} = 6,2 Hz), δ = -116.79 ppm (d, 1F, ³J_{C-F} = 6,2 Hz).

N- (2-ethoxy-2-oxoethyl), N-(3-chloro-4-fluorophenyl)- (1-2-ethoxy-2-oxoethyl -2-oxo-1,2-dihydroquinoline-4)-carboxamide: 17

Yield (%) = 80 %; mp > 473 K; ¹H NMR (300 MHz, CDCl₃): 1.19 (t, 3H, ³J_{H-H} = 7.2 Hz, CH₃), 1.36 (t, 3H, ³J_{H-H} = 7.2 Hz, CH₃), 4.18 (q, 2H, ³J_{H-H} = 7.2 Hz, CH₂), 4.33 (q, 2H, ³J_{H-H} = 7.2 Hz, CH₂), 4.59 (s, 2H, OCH₂), 5.00 (s, 2H, OCH₂), 6.51 (s, 1H, CH_{arom}), 6.90-8.01 (m, 7H, CH_{arom}). ¹³C NMR (75 MHz, CDCl₃): 168.36 (C=O), 167.62 (C=O), 167.06 (C=O), 160.55 (C=O), 157.61 (d, Cq, ¹J_{C-F} = 250.73 Hz), 145.00-139.35 (Cq-Cq), 138.16 (d, Cq, ⁴J_{C-F} = 3.75 Hz), 131.72 (CH_{arom}), 129.82 (CH_{arom}), 127.71 (d, CH_{arom}, ³J_{C-F} = 7.5 Hz), 127.30 (CH_{arom}), 123.15 (CH_{arom}), 121.92 (CH_{arom}), 121.92 (d, Cq, ³J_{C-F} = 18.75 Hz), 119.43 (CH_{arom}), 117.80 (CH_{arom}), 117.35 (d, CH_{arom}, ²J_{C-F} = 21.75 Hz), 114.02 (CH_{arom}), 61.89 (CH₂), 61.11 (CH₂), 52.03 (CH₂), 44.14 (CH₂), 14.22 (CH₃), 14.02 (CH₃). ¹⁹F NMR (282 MHz, CDCl₃): δ = -121.74 ppm.

N- (2-ethoxy-2-oxoethyl), (3-(trifluoromethyl)phenyl)- (1-2-ethoxy-2-oxoethyl -2-oxo-1,2-dihydroquinoline-4)-carboxamide: 18

Yield (%) = 79 % ; mp > 433,15 K; ¹H NMR (300 MHz, CDCl₃): 1.14 (t, 3H, ³J_{H-H} = 7.2 Hz, CH₃), 1.32 (t, 3H, ³J_{H-H} = 7.2 Hz, CH₃), 4.13 (q, 2H, ³J_{H-H} = 7.2 Hz, CH₂), 4.31 (q, 2H, ³J_{H-H} = 7.2 Hz, CH₂), 4.61 (s, 2H, OCH₂), 4.93 (s, 2H, OCH₂), 6.46 (s, 1H, CH), 7.00-7.51 (m, 7H, CH_{arom}), 8.00-8.03 (m, 1H, CH_{arom}). ¹³C NMR (75 MHz, CDCl₃): 168.34 (C=O), 167.57 (C=O), 167.08 (C=O), 160.51 (C=O), 145.87 (Cq), 145.06-139.28 (Cq-Cq), 131.69 (CH_{arom}), 130.85 (CH_{arom}), 130.29 (CH_{arom}), 129.21 (2 CH_{arom}), 127.29 (CH_{arom}), 125.15 (q, Cq, ³J_{C-F} = 3.75 Hz), 124.21 (q, Cq, ³J_{C-F} = 3.75 Hz), 123.12 (CH_{arom}), 119.50 (CH_{arom}), 117.80 (Cq), 113.95 (CH_{arom}), 62.01 (CH₂), 61.75 (CH₂), 51.35 (CH₂), 43.81 (CH₂), 14.16 (CH₃), 14.00 (CH₃). ¹⁹F NMR (282 MHz, CDCl₃): δ = -61.72 ppm (3F, CF₃).

2.3. Single crystal X-ray diffraction

2.3.1. Crystal structures of the 2-oxo-1,2-dihydroquinoline derivatives (**10**, **11**, **15** and **18**)

The crystallographic analyses of the 2-oxo-1,2-dihydroquinoline derivatives (**10**, **11**, **15** and **18**), obtained by cyclocondensation, substituted anilines and alkylation reactions, confirm the structures of the compounds (Fig.1 and Table 1). It is interesting to note that compound **11** crystallizes in the triclinic system ($P\bar{1}$), compounds **15** and **18** crystallize in the monoclinic system ($I2/a$) and compound **10** crystallizes in the orthorhombic system ($Pbca$). The crystallographic data have been assigned to CCDC deposition numbers (see Table 1)

2.4. Computational details

Density Functional Theory (DFT) methods are very important owing to cost of computations and reliable results for complex molecules in quantum chemistry. In this method, frequently Becke-3-Lee-Yang-Parr (B3LYP) functionals are used [27]. For the molecular orbital computations, the 6-311G(d,p) basis set was selected and the Gaussian 09W software package [28] was used. Firstly, molecular optimizations of compounds **10**, **11**, **15** and **18** were carried out using the atomic coordinates in the CIF files, obtained from the crystallographic studies, and other geometry optimized computations were made based on their optimized structures. In order to visualize the intermolecular interactions in the crystals of compounds **10**, **11**, **15** and **18** Hirshfeld surface (HS) analyses were carried out by using CrystalExplorer17.5 [29]. Also, in this study, Highest Occupied Molecular Orbital (HOMO) and Lowest Unoccupied Molecular Orbital (LUMO) analyses for compounds **10**, **11**, **15** and **18** were mostly formed from π and π^* molecular orbitals of the aromatic groups, respectively. The ^1H - and ^{13}C -NMR chemical shifts of compounds **10**, **11**, **15** and **18** were calculated with the Gauge-Including Atomic Orbital (GIAO) approach by using the B3LYP/6-311G(d,p) basis set and compared with the experimental NMR spectra in a DMSO- d_6 solvent. Finally, molecular docking studies between compounds **10**, **11**, **15** and **18** and inter-molecular interactions between the macromolecules (PDB ID: 1M17) were carried out employing the AutoDock Vina free software program [43].

2.5. Molecular geometric properties

The geometry optimized molecular structures along with the numbering (scheme 2) for compounds **10**, **11**, **15** and **12** are shown in Fig. 2. The geometry optimized bond lengths and angles of the title molecules were calculated using the B3LYP functional along with the 6-311G(d,p) basis set. Some important and selected theoretical and experimental geometric parameters are listed in Table 2. From Table 2, we can see that there are some mismatches

between the experimental and geometry optimized molecular structures. It is noted that the optimized structures are calculated in the gas phase, while the experimental structures are obtained from the data collected in the solid phase. In the oxo-dihydroquinoline group, the O1=C1 bond length was calculated as 1.22430 Å (for compound **10**), 1.22289 Å (O1A=C1A) (for compound **11**), 1.22337 Å (for compound **15**) and 1.22326 Å (for compound **18**) with the B3LYP/6-311G(d,p) functional/basis set. These bonds were determined experimentally as 1.234(3) Å (for compound **10**), 1.231(2) Å (O1A=C1A) (for compound **11**), 1.226(3) Å (for compound **15**) and 1.230(3) Å (for compound **18**). The corresponding bond (O1=C9 according to the reported numbering scheme) has been calculated as 1.231 Å, 1.230 Å and 1.228 Å with B3LYP/6-311++G(d,p) for ethyl 1-ethyl-2-oxo-1,2-dihydroquinoline-4-carboxylate and ethyl-6-chloro-1-ethyl-2-oxo-1,2-dihydroquinoline-4-carboxylate [30], respectively. On the other hand, the N1—C1 and N1—C9 bond lengths were calculated as 1.40521 Å and 1.39253 Å (for compound **10**), 1.39376 Å and 1.39376 Å (for compound **11**), 1.40882 Å and 1.39342 Å (for compound **15**) and 1.40895 Å and 1.39311 Å (for compound **18**), respectively, with the B3LYP/6-311G(d,p) functional/basis set. The experimentally determined corresponding bond lengths were 1.383(3) Å and 1.393(3) Å (for compound **10**), 1.389(3) Å and 1.397(3) Å (for compound **11**), 1.382(2) Å and 1.390(3) Å (for compound **15**) and 1.380(2) Å and 1.392(3) Å (for compound **18**), respectively. In the literature [30], these bond lengths are very compatible with our results. We may also pay attention to some important bond angles in the oxo-dihydroquinoline group. The bond angles C1—N1—C9, O1—C1—N1 and O1—C1—C2 were calculated as 122.7(2)°, 120.9(2)° and 122.9(2)°, respectively, (for compound **10**), 123.16(18)°, 121.2(2)° and 122.9(2)°, respectively, (for compound **11**), 123.48(16)°, 121.34(19) and 123.13(18)°, respectively, (for compound **15**) and 123.59(16)°, 121.35(18)° and 123.16(18)°, respectively (for compound **18**). These values are smaller than 120° because of the presence of the oxo-dihydroquinoline ring as explained in the literature [30]. For example, in the heterocyclic 4-hydroxy-2-oxo-1,2-dihydroquinoline-7-carboxylic acid molecule [31], the bond angles C1—C2—C3 and C2—C3—C4 were reported as 119.66° and 119.4°, respectively. The C1—N1—C9, O1—C1—N1 and O1—C1—C2 bond angles were calculated as 123.04954°, 121.40406° and 122.94433°, respectively (for compound **10**), 123.44171°, 121.44592° and 123.24597°, respectively (for compound **11**), 123.39328°, 121.17736 and 123.39068°, respectively (for compound **15**) and 123.46631°, 121.22491° and 123.39693°, respectively (for compound **18**), with the B3LYP/6-311G(d,p) functional/basis. These bond lengths and angles are generally compatible with the corresponding values in similar structures [30-31].

2.6. HOMO-LUMO Analysis

The Highest Occupied Molecular Orbital (HOMO) and the Lowest Unoccupied Molecular Orbital (LUMO) parameters are very important to understand aspects of the quantum chemistry mechanism and the chemical reaction pathways. Usually, HOMO is known as a donor, while LUMO is known as an acceptor [32-33]. While HOMO energy is related to the ionization potential, LUMO energy is related to the electron activation. Other important parameters are the energy gap values of the compounds. The energy differences between HOMO and LUMO are called the energy band gaps ($\Delta E = E_{\text{LUMO}} - E_{\text{HOMO}}$), and for the stabilities of the structures they are very crucial, where the higher-gap energy is more stable than the lower-gap energy. Additionally, the HOMO–LUMO gaps for compounds **10**, **11**, **15** and **18** were calculated as 4.2273 eV, 4.3394 eV, 4.3675 eV and 4.2972 eV, respectively. From these results, we can conclude that the sum of the electronic and zero-point energies of compound **10** is relatively low (the most stable structure according to the energy results) and its gap is small. Furthermore, by using HOMO and LUMO energy values we can calculate the other important parameters such as the Ionization potential $= I = -E_{\text{HOMO}}$; the electron affinity $= A = -E_{\text{LUMO}}$; the chemical hardness $= \eta = (I - A)/2$; the electrophilicity index, $\omega = \mu^2/2\eta$ and softness, $\zeta = 1/2\eta$. These parameters have been calculated and given in Table 3. The HOMO's and LUMO's (HOMO-LUMO cloud distributions) (**Fig. 3**) were obtained and simulated from the optimized molecular geometries using the .chk files in the gas phase at the B3LYP/6-311G(d,p) functional/levels.

2.7. NMR Analyses

Theoretical studies on geometric structures, NMR chemical shifts and HOMO-LUMO analyses for compounds **10**, **11**, **15** and **18** were performed by the B3LYP functional [27-34] method by using the 6-311G(d,p) basis set. Gaussian 09W software [28] was used to compute the aforementioned electronic structure properties, while GaussView5 software [35] was used to monitorize these computed features. The initial structures for all computations were carried out using the atomic coordinates from the CIF files, obtained from the crystallographic studies.

The optimized geometrical parameters for compounds **10**, **11**, **15** and **18** were obtained in the gas phase. For the theoretical NMR chemical shift analyses, all molecular structures were optimized within chloroform with the IEF-PCM model [36]. Then, ^{13}C - and ^1H -NMR chemical shifts for compounds **10**, **11**, **15** and **18** were found with the GIAO method [37] by using the same computational procedures and the same solvation model parameters. The

NMR isotropic chemical shift values were calculated *via* the equation $\delta_{iso}^x = \sigma_{iso}^{TMS} - \sigma_{iso}^x$. [where δ_{iso}^x is the isotropic chemical shift of any atom within the compound, σ_{iso}^{TMS} is the isotropic absolute shielding value of carbon (average of four) and hydrogen (average of twelve) atoms within TMS and σ_{iso}^x is the isotropic absolute shielding value of any atom within the compound]. The isotropic absolute shielding values computed at the B3LYP/6-311G(d,p) functional/levels within chloroform of TMS (tetramethyl silane) were found as 32.00 ppm for protons and 184.9 ppm for carbons. The experimental and computed ^1H - and ^{13}C -NMR chemical shifts are given in Tables 4 and 5. Generally, the observed and calculated ^1H - and ^{13}C -NMR chemical shifts are in a very good agreement with the corresponding literature values [31, 38]. There are fourteen ^{13}C - and fifteen ^1H -NMR chemical shifts for the title molecules that we can locate precisely as may be seen in Tables 4 and 5.

2.8. Hirshfeld surface analyses

Hirshfeld surface analysis may be used to research all of the possible inter-molecular interactions *via* contact atoms (donor and acceptor groups) within the crystal packing of any crystalline compound. The normalized contact distance function (d_{norm}) may be used to analyze the close contact interaction distances (the inter-molecular interaction distances between donor and acceptor groups in effective sites of molecular groups within an interaction) on its related 3D d_{norm} Hirshfeld surfaces. The 3D d_{norm} surfaces and their related 2D fingerprint graphics were depicted *via* the Crystal Explorer program software used to investigate the Hirshfeld surfaces of compounds **10**, **11**, **15** and **18** (Hirshfeld, 1977; Wolff, Grimwood, McKinnon, Turner, Jayatilaka & Spackman, 2012; Spackman & Jayatilaka, 2009; M.A. Spackmann, McKinnon & Jayatilaka, 2008) [39-42].

$$d_{norm} = \frac{d_i - r_i^{vdW}}{r_i^{vdW}} + \frac{d_e - r_e^{vdW}}{r_e^{vdW}}$$

where d_i is the length from a point on the surface to the nearest inside nucleus, and d_e is the length from a point on the surface to the nearest external nucleus. They are represented by the red (for short distances), blue (for medium distances) and green (for long distances) regions on their mapped surfaces. Likewise, d_{norm} is the normalized contact distance depending upon d_i and d_e distances and the van der Waals radius (r^{vdW}). Its 3D related surface is mapped by the red, white and blue colors. The red (negative value) and blue (positive value) regions indicate inter-molecular distances for contacts shorter and longer than the sum of r^{vdW} , respectively. Moreover, the white regions (zero value) represents the inter-molecular distances for contacts close/equal to the sum of r^{vdW} .

The depicted 3D d_{norm} surfaces and their reduced related 2D fingerprint histograms are given in Figs. 4 and 5, respectively. The presence of the red points on the 3D d_{norm} surfaces of compounds **10**, **11**, **15** and **18** indicates the existence of inter-molecular interactions. The interactions with major contributions within the crystal packings of all four compounds are due to the van der Waals interactions of the H \cdots H species with the percentage values of 43.9% (for compound **10**), 39.1% (for compound **11**), 53.9% (for compound **15**) and 39.1% (for compound **18**). For compounds **10**, **11**, **15** and **18**, the O \cdots H/H \cdots O interactions were obtained with the percentage values of 14.6%, 17.5%, 28.5% (the second major contribution for compound **15**) and 21.96% (the second major contribution for compound **18**), respectively, while the C \cdots H/H \cdots C and C \cdots C species indicating the existence of the C-H \cdots π and $\pi\cdots\pi$ interactions within the crystal packings were computed with the percentage values of 6.2%, 35.7% (the second major contribution for compound **11**), 11.8% and 11.3% and 6.6%, 5.9%, 2.8% and 2.7%, respectively. The second and third major contributions in compounds **10** and **18** are resulted from F \cdots H/H \cdots F interactions with the percentage values of 22.5% and 17.7%, respectively. Finally, the F \cdots F and F \cdots O/O \cdots F interaction species within compounds **10** and **18** were found with the percentage values of 3.3% and 3.6%, respectively.

2.9. Molecular Docking Studies

A molecular docking study was performed to determine the existence of the inter-molecular interactions between the target protein (PDB ID: 1M17) and the ligand compounds (**10**, **11**, **15** and **18**). The molecular docking analyses were carried out by using the AutoDock Vina program [43]. The high-resolution crystal structure of macromolecule 1M17 was taken from the RCSB Protein Data Bank website [44]. The macromolecule 1M17 is formed by interactions among a protein group (Epidermal Growth Factor Receptor (EGFR)), a ligand compound ([6,7-bis(2-methoxy-ethoxy)quinazoline-4-yl]-(3-ethynylphenyl)amine) and water molecules. For docking protocol, the target protein EGFR was obtained by deleting the ligand compound and water molecules mentioned within the macromolecule 1M17, while the initial molecular geometries of the ligand compounds (**10**, **11**, **15** and **18**) were obtained by the single crystal X-ray diffraction studies. The PDB files of the target protein (EGFR) and the ligand compounds were created by using DS Visualizer (Discover Studio Visualizer) program software (Dassault Systems BIOVIA) [45]. Moreover, the visualizations of the inter-molecular interactions between the ligand compounds and the target protein were depicted by using DS Visualizer program software. As in Ref. 44, the molecular docking analysis in this study was done to put forth the activity and inter-molecular interaction profile of the compounds within this study against EGFR.

The ligand compounds (**10**, **11**, **15** and **18**) were docked into space containing the active site region of target protein 1M17. The active sites of this target protein are residues LEU694, ALA719, LEU764, THR766, GLN767, LEU768, MET769, PRO770, PHE771, GLY772, LEU820, THR830 and ASP831. The dimensions of the research space volume were decided as (40 Å × 42 Å × 44 Å) of the grid size (spacing = 0.375 Å). The position of this research space volume was set as 23.0, 0.5 and 53.6 for the x, y and z coordinates of the center. According to the results of the molecular docking analysis, the obtained binding affinities and RMSD values for ten different poses of the ligand compounds docked onto macromolecule 1M17 are listed in Table 6. In order to be able to talk about an acceptable molecular docking analysis, the calculated RMSD values are expected to be less than 2 Å [46]. The best binding affinity values for all four ligand compounds docked onto macromolecule 1M17 were computed as -8.40 kcal/mol (for compound **10**), -8.80 kcal/mol (for compound **11**), -7.80 kcal/mol (for compound **15**) and -8.60 kcal/mol (for compound **18**). According to these binding affinity results, compound **11** may be an effective docking material for epidermal growth factor receptor tyrosine kinase. The 2-D and 3-D visuals of the inter-molecular interactions for the best binding poses of the ligand compounds docked into macromolecule 1M17 can be seen in Fig. 6. Moreover, Table 7 shows the inter-molecular hydrogen bond interactions and their distances between the compounds **10**, **11**, **15** and **18** with macromolecule 1M17. The hydrogen bond formation was taken to connect between the ketone =O atom in 4-carboxamide of the ligand compound **10** and the OH group in the residue THR830 of the target protein with a value of 3.18 Å of the interaction distance. Similarly, a $\pi\cdots\pi$ stacking interaction was formed between the delocalized π -electrons of the 2-oxo-1,2-dihydroquinoline ring of compound **10** with the delocalized π -electrons of the phenyl ring in residue PHE699 of the macromolecule. The conventional hydrogen bond interaction for ligand compound **11** was formed between an =O atom in the 2-oxo-1,2-dihydroquinoline ring and the OH group in the residue THR830 is at a distance of 2.90 Å, while the $\pi\cdots\pi$ stacking interaction was taken over by the delocalized π -electrons of the phenyl rings in the ligand and residue of PHE699. Four conventional hydrogen bond interactions were obtained between ligand compound **15** and the macromolecule. Three interactions were formed between the oxygen atoms in 2-ethoxy-2-oxoethyl of the ligand compound and the polar groups in the residues of THR766, THR830 and CYS751 with distances of 2.98 Å, 2.97 Å and 3.37 Å, respectively, while one hydrogen bond interaction was found between an =O atom in the 2-oxo-1,2-dihydroquinoline ring and cationic -NH₃

group of residue LYS721. Finally, the hydrogen bond interactions between the oxygen atoms of 2-ethoxy-2-oxoethyl in ligand compound **18** and the OH groups of the residues THR830 and THR766 in the macromolecule 1M17 were recorded at 2.79 Å and 3.00 Å, respectively. The other interaction species [halogen (fluorine), π -anion, π -sigma, π -sulfur, alkyl and π -alkyl] for all four compounds are shown in Fig. 6 along with their interaction distances.

3. Conclusion

These studies reflect that 2-oxo-1,2-dihydroquinoline is a nucleus likely to be used in a drug discovery area and medicines. Moreover, in this work, we report the syntheses of novel 2-oxo-1,2-dihydroquinoline derivatives: **7-18**. The structures of four compounds 10, 11, 15 and 18 have been identified by using single crystal X-ray crystallography and spectroscopic techniques. The theoretical approach used in this work allows a relatively good reproduction of X-ray geometrical parameters, spectral data, and ^1H -, ^{13}C - and ^{19}F -NMR chemical shifts. Hirshfeld surfaces were employed to confirm the existence of intermolecular interactions in compounds 10, 11, 15 and 18. The experimental spectroscopic data were well reproduced by using quantum chemical DFT theoretical calculations and in silico-based molecular docking studies.

Acknowledgements

Author would like JTM thanks Tulane University for support of the Tulane Crystallography Laboratory.

Abbreviations

DMSO-dimethylsulfoxide
HOMO-highest occupied molecular orbital
LUMO-lowest unoccupied molecular orbital
NMR- Nuclear magnetic resonance
PDB-Protein Data Bank
DFT- Density Functional Theory
DCM- Dichloromethane

References

1. Alcaide, B.; Almendros, P.; Aragoncillo, C.; Highly reactive 4-membered ring nitrogen-containing heterocycles: Synthesis and properties. *Curr. Opin. Drug Discov. Dev*, **2010**, 13, 685–597.
2. Jones, S. B.; Simmons, B.; Mastracchio, A.; MacMillan, D. W. C.; Collective synthesis of natural products by means of organocascade catalysis. *Nature*, **2011**, 475(7355), 183–188.

3. Leshner, G. Y.; Froelich, E. J.; Gruett, M. D.; Bailey, J. H.; Brundage, R. P.; 1,8-Naphthyridine Derivatives. A New Class of Chemotherapeutic Agents. *Journal of Medicinal and Pharmaceutical Chemistry*, **1962**, 5(5), 1063–1065.
4. Trivedi, A.; Dodiya, D.; Surani, J.; Jarsania, S.; Mathukiya, H.; Ravat, N.; V.; Shah Facile one-pot synthesis and antimycobacterial evaluation of pyrazolo[3,4d]pyrimidines. *Archiv Pharmazie*. **2008**, 341, 435-439.
5. Dlugosz, A.; & Dus, D.; Synthesis and anticancer properties of pyrimido[4,5-b]quinolines. *Farmaco*. **1996**, 51 (5), 364-374.
6. Šamšulová, V.; Poláková, M.; Horák, R.; Šedivá, M.; Hradil P.; Synthetic approach to novel glycosyltriazole-3-hydroxyquinolone conjugates and their antimicrobial properties. *J. Mol. Struct.* **2019**, 1177, 16-25.
7. El-Sayed, O.A.; Al-Bassam, B.A.; Hussein, M.E.; Synthesis of some novel quinoline-3-carboxylic acids and pyrimidoquinoline derivatives as potential antimicrobial agents. *Archiv Pharmazie*. **2002**, 335, 403-410.
8. El-Sayed, O.A.; El-Bieh, F.M.; El-Aqeel, S.I.; Al-Bassam, B.A.; Hussein; M.E.; Novel 4-aminopyrimido[4,5-b]quinoline derivatives as potential antimicrobial agents. *Bollettino Chimico Farmaceutico*. **2002**, 141, 461-465.
9. Gayathri, K.; Radhika, R.; Shankar, R.; Malathi, M.; Savithiri, K.; Sparkes, H.A.; Howard, J.A.K.; Mohan. P.S.; Comparative theoretical and experimental study on novel tri- quinoline system and its anticancer studies, *J. Mol. Struct.* **2017**, 1134, 770-780.
10. El-Sayed, O.A.; Al-Turki, T.M.; Al-Daffiri, H.M.; Al-Bassam, B.A.; Hussein, M.E.; Tetrazolo[1,5-a] quinoline derivatives as anti-inflammatory and antimicrobial agents. *Bollettino Chimico Farmaceutico*. **2004**, 143, 227-238.
11. Gavrilov, M.Y.; Mardanova, L.G.; Kolla, V.E.; Konshin. M.E.; Synthesis, antiinflammatory and analgesic activities of 2-aryl-amino-5,6,7,8-tetrahydroquinoline-3-carboxamides. *Pharmaceut. Chem. J.* **1988**, 22, 554-556.
12. Lilienkampf, A.; Mao, J.; Wan, B.; Wang, Y.; Franzblau, S. G.; Kozikowski, A. P.; Structure-activity relationships for a series of quinoline-based compounds active against replicating and nonreplicating Mycobacterium tuberculosis. *J. Med. Chem.* **2009**, 52, 2109-2118.
13. Mai, A.; Rotili, D.; Tarantino, D.; Nebbioso, A.; Castellano, S.; Sbardella. G.; Identification of 4-hydroxyquinolines inhibitors of p300/CBP histone acetyltransferases. *Bioorg. Med. Chem. Lett.* **2009**, 19, 1132-1135.
14. Rano, T.A.; Mc Master, E.S.; Pelton, P.D.; Yang, M.; Demarest, K.T.; Kuo. G.H.; Design and synthesis of potent inhibitors of cholesteryl ester transfer protein (CETP) exploiting a 1,2,3,4-tetrahydroquinoline platform. *Bioorg. Med. Chem. Lett.* **2009**, 19, 2456-2460.
15. Mahamoud, A.; Chevalier, J.; Davin-Regli, A.; Barbe, J.; Quinoline derivatives as promising inhibitors of antibiotic efflux pump in multidrug resistant Enterobacter aerogenes isolates. *Curr. Drug. Target.* **2006**, 7, 843-847.
16. Muruganantham, N.; Sivakumar, R.; Anbalagan, N.; Gunasekaran, V.; Leonard, J.T.; Synthesis, anticonvulsant and antihypertensive activities of 8-substituted quinoline derivatives. *Biol. Pharm. Bull.* **2004**, 27, 1683-1687.

17. Maguire, M.P.; Sheets, K.R.; Mc Vety, K.; Spada, A.P.; Zilberstein. A.; A new series of PDGF receptor tyrosine kinase inhibitors: 3-substituted quinoline derivatives. *J. Med. Chem.* **1994**, *37*, 2129-2137.
18. Wilson, W.D.; Zhao, M.; Patterson, S.E.; Wydra, R.L.; Janda, L.; Streckowski, L.; Schinazi. R.F.; Design of RNA interactive anti-HIV agents: unfused aromatic intercalators. *Med. Chem. Res.* **1992**, *2*, 102-110.
19. Chakraborty, B.; Dutta, D.; Mukherjee, S.; Das, S.; Maiti. N.C.; Synthesis and biological evaluation of a novel betulinic acid derivative as an inducer of apoptosis in human colon carcinoma cells (HT-29). *Eur J. Med. Chem.* **2015**, *102*, 93-105.
20. Li, L.N.; Zhang, H.D.; Yuan, S.J.; Yang, D.X.; Wang, L.; Sun. Z.X.; Differential sensitivity of colorectal cancer cell lines to artesunate is associated with expression of β -catenin and E-cadherin. *Eur. J. Pharmacol.* **2008**, *588*, 1-8.
21. Kouznetsov, V.V.; Rojas Ruíza, F.A.; Vargas Méndeza, L.Y.; Gupta. M. P.; Simple C-2-Substituted Quinolines and their Anticancer Activity. *Lett. Drug. Des. Discov.* **2012**, *9*, 680-686.
22. Achan, J.; Talisuna, A.O.; Erhart, A.; Yeka, A.; Tibenderana, J.K.; Baliraine, F.N.; Rosenthal, P.J.; D'Alessandro. U.; Quinine, an old anti-malarial drug in a modern world: Role in the treatment of malaria. *Malar J.*, **2011**, *10*, 1-12.
23. Joomyung, V. J.; Petersson, E. J.; Chenoweth M. D.; Rational Design and Facile Synthesis of a Highly Tunable Quinoline-Based Fluorescent Small-Molecule Scaffold for Live Cell Imaging. *J. Am. Chem. Soc.* **2018**, *140*(30), 9486-9493.
24. Chanda, T.; Verma, R.K.; Singh, M.S.; InCl₃-driven regioselective synthesis of functionalized/annulated quinolines: Scope and limitations. *Chem. Asian J.*, **2012**, *7*, 778–787.
25. Filali Baba, Y.; Kandri Rodi, Y. ; Misbahi, K.; Chahdi Ouazzani, F.; Kerbal, A.; Essassi, E. M.; Synthesis and reactivity of new heterocyclic systems derived from quinoline, *J. Mar. Chim. Heterocycl.* **2014**, *13*, 72-80.
26. Filali Baba, Y.; Hokelek, T.; Kaur, M.; Jasinski, J.; Sebbar, N. K.; Kandri Rodia. Y.; Crystal structure, Hirshfeld surface analysis and DFT studies of ethyl 2-{4-[(2-ethoxy-2-oxoethyl)(phenyl)carbamoyl]-2-oxo-1,2-dihydroquinolin-1yl}acetate. *Acta Cryst.* **2019**, *E75*, 1753–1758.
27. Becke. A.D.; Density functional thermochemistry III. The role of exact exchange. *J. Chem. Phys.* **1993**, *98*, 5648-5652.
28. Frisch, M.J.; Trucks, G.; Schlegel, H.B.; Scuseria, G.; Robb, M.; Cheeseman, J.; Scalmani, G.; Barone, V.; Mennucci, B.; Petersson, G.; Gaussian 09, revision A. 1, Gaussian Inc. Wallingford CT, **2009**, *27*, 34.
29. Turner M.;, Mc Kinnon, J.; Wolff, S.; Grimwood, D.; Spackman, P.; Jayatilaka, D.; Spackman, M.; CrystalExplorer17, University of Western Australia,, <http://hirshfeldsurface.net>. **2017**.
30. Filali Baba, Y.; Sert, Y.; Kandri Rodi, Y.; Hayani, S.; Mague, J.T.; Prim, D.; Marrot, J.; Ouazzani Chahdi, F.; Sebbar, N. K.; Essassi. E. M.; Synthesis, crystal structure, spectroscopic characterization, Hirshfeld surface analysis, molecular docking studies and DFT calculations, and antioxidant activity of 2-oxo-1,2-dihydroquinoline-4-carboxylate derivatives. *Journal of Molecular Structure.* **2019**, *1188*, 255-268.

31. Ulahannan, R.T.; Panicker, C.Y.; Varghese, H.T.; Van Alsenoy, C.; Musiol, R.; Jampilek, J.; Anto, P.; Spectroscopic (FT-IR, FT-Raman) investigations and quantum chemical calculations of 4-hydroxy-2-oxo-1, 2-dihydroquinoline-7-carboxylic acid. *Spectrochim. Acta A*. **2014**, 121, 404-414.
32. Fukui K.; Role of frontier orbitals in chemical reactions. *Science*. **1982**, 218, 747-754.
33. Parr, R.G.; Pearson. R.G.; Absolute hardness: companion parameter to absolute electronegativity, *J. Am. Chem. Soc.* **1983**, 105, 7512-7516.
34. Lee, C.; Yang, W.; Parr. R.G.; Development of the Colle-Salvetti correlation-energy formula into a functional of the electron density, *Phys. Rev. B*, **1988**, 37(2), 785-789.
35. Dennington, R.; Keith, T.; Millam J.; GaussView, Version 5, Shawnee Mission KS, Semichem Inc. **2009**.
36. Cancès, E.; Mennucci, B.; Tomasi, J.; A New Integral Equation Formalism for the Polarizable Continuum Model: Theoretical Background and Applications to Isotropic and Anisotropic Dielectrics, *J. Chem. Phys.* **1997**, 107(8), 3032-3041.
37. London F.; Théorie Quantique des Courants Interatomiques dans les Combinaisons Aromatiques, *J. Phys. Radium*. **1937**, 8(10), 397-409.
38. Al-Otaibi, J.S.; Al-Wabli. R.I.; Vibrational spectroscopic investigation (FT-IR and FT-Raman) using ab initio (HF) and DFT (B3LYP) calculations of 3-ethoxymethyl-1, 4-dihydroquinolin-4-one. *Spectrochim. Acta A*. **2015**, 137, 7-15.
39. Hirshfeld, F.L.; Bonded-Atom Fragments for Describing Molecular Charge Densities, *Theor. Chim. Acta*. **1977**, 44(2), 129-138.
40. Wolff, S.K.; Grimwood, D.J.; McKinnon, J.J.; Turner, M.J.; Jayatilaka, D.; Spackman. M.A.; CrystalExplorer, Version 3.1, **2012**.
41. Spackman, M.A.; Jayatilaka, D.; Hirshfeld Surface Analysis, *Cryst. Eng. Comm.* **2009**, 11, 19-32.
42. Spackmann, M.A.; McKinnon, J.J.; Jayatilaka, D; Electrostatic Potentials Mapped on Hirshfeld Surfaces Provide Direct Insight into Intermolecular Interactions in Crystals, *Cryst. Eng. Comm.* **2008**, 10, 377-388.
43. Trott, O.; Olson. A.J.; *J. Comput. Chem.* **2010**, 31(2), 455-461.
44. Stamos, J.; Sliwowski, M.X.; Eigenbrot, C.; Structure of the Epidermal Growth Factor Receptor Kinase Domain Alone and in Complex with a 4-Anilinoquinazoline Inhibitor, *J. Biol. Chem.* **2002**, 277(48), 46265-46272.
45. Dassault Systèmes BIOVIA, Discovery Studio Modeling Environment, Release 2017, San Diego, Dassault Systèmes, **2016**.
46. Kramer, B.; Rarey, M.; Lengauer, T.; Evaluation of the FLEXX Incremental Construction Algorithm for Protein–Ligand Docking. *Proteins: Struct. Funct. Genet.* **1999**, 37(2), 228-241.

Figure Captions

Fig. 1 ORTEP drawings of compounds 10, 11, 15 and 18 showing atom numbering schemes and displacement ellipsoids drawn at the 50% probability level.

Fig. 2 Geometry optimized theoretical structures for compounds 10, 11, 15 and 18 using the B3LYP functional at the 6-311G(d,p) level of theory.

Fig. 3 HOMO-LUMO molecular orbital cloud distributions for compounds 10, 11, 15 and 18 calculated at the B3LYP/6-311G(d,p) level of theory. HOMO-LUMO energy levels and gap calculations are displayed in eV's.

Fig. 4 Complimentary views of the three-dimensional surfaces for compounds 10, 11, 15 and 18 plotted over d_{norm} in the range -0.35 to 1.34 a.u.

Fig. 5 A view of the two-dimensional fingerprint plots for compounds 10, 11, 15 and 18 showing (a) all interactions and separated into (b) H...H and/or, (c) O...H/H...O and/or, (d) H...C/C...H and/or, (e) C...H/H...C and/or, (f) C---C and/or, (g) F...H/H...F and/or, (h) F...O/O...F interactions. The d_i and d_e values are closest internal and external distances (in Å) from given points on the Hirshfeld surface contacts.

Fig. 6 A view of the 2-D and 3-D visuals of the intermolecular interactions for the best binding poses of ligand compounds 10, 11, 15 and 18 docking with the residues of macromolecule 1M17. Intermolecular hydrogen bond interactions and their distances between compounds 10, 11, 15 and 18 with macromolecule 1M17 are given in Table 7.

	Compound 10	Compound 11	Compound 15	Compound 18
Chemical formula	C ₂₁ H ₁₉ F ₃ N ₂ O ₂	2(C ₂₂ H ₁₆ N ₂ O ₂)	C ₂₄ H ₂₄ N ₂ O ₆	C ₂₅ H ₂₃ F ₃ N ₂ O ₆
CCDC Deposition Number	1954732	19547664	1959642	1954744
Recrystallization solvent	hexane / DCM (3/1)			
M_r	388.38	680.73	436.45	504.45
Crystal system, space group	orthorhombic, <i>P bca</i>	triclinic, <i>P</i> $\bar{1}$	monoclinic, <i>I</i> 2/a	monoclinic, <i>I</i> 2/a
Temperature (K)	293	293	293	293
a, b, c (Å)	17.1196 (5), 8.0328 (3), 27.6991 (6)	10.7160 (7), 11.3615 (7), 16.5479 (8)	16.9368 (5), 15.4130 (4), 18.4562 (6)	16.8605 (4), 16.2855 (4), 18.5440 (5)
α, β, γ (°)		81.273 (5), 85.833 (5), 64.001 (7)	109.254 (4)	110.389 (3)
V (Å³)	3809.1 (2)	1789.8 (2)	4548.4 (3)	4772.8 (2)
Z	8	2	8	8
Radiation type	Cu K α	Cu K α	Cu K α	Cu K α
μ (mm⁻¹)	0.91	0.66	0.76	0.99
Data collection				
Diffractometre	Xcalibur, Eos, Gemini	Rigaku Oxford Diffraction, Gemini	Rigaku Oxford Diffraction, Gemini	Rigaku Oxford Diffraction, Gemini
No. Of measured, independent and observed [<i>I</i> > 2σ(<i>I</i>)] reflections	26345, 3682, 2879	12436, 6721, 4730	8768, 4330, 3266	9504, 4549, 3642
R_{int}	0.037	0.028	0.018	0.017
(sinθ/λ)_{max} (Å⁻¹)	0.615	0.615	0.613	0.613
Refinement				
R[F² > 2σ(F²)], wR(F²), S	0.068, 0.230, 1.06	0.053, 0.160, 1.02	0.051, 0.161, 1.05	0.053, 0.170, 1.03
No. Of reflections	3682	6721	4330	4549
No. Of parametres	265	469	291	344
$\Delta\rho_{max}, \Delta\rho_{min}$ (e Å⁻³)	0.54, -0.40	0.19, -0.17	0.32, -0.18	0.30, -0.32

Bond angles (°)			Bond lengths (Å)		
Optimized bond angles	X-Ray	DFT/B3LYP 6-311 G(d,p)	Optimized bond lengths	X-Ray	DFT/B3LYP 6-311 G(d,p)
Compound 10					
C1—N1—C9	122.7(2)	123.04954	F1—C17	1.398(8)	1.34989
C1—N1—C20	116.9(2)	115.59882	F2—C17	1.305(7)	1.35395
C9—N1—C20	120.3(2)	121.32950	F3—C17	1.307(6)	1.35062
C10—N2—C11	124.3(2)	124.06661	O1—C1	1.234(3)	1.22430
C10—N2—C18	117.6(2)	116.52548	O2—C10	1.224(3)	1.22040
C11—N2—C18	117.8(2)	118.73550	N1—C1	1.383(3)	1.40521
O1—C1—N1	120.9(2)	121.40406	N1—C9	1.393(3)	1.39253
O1—C1—C2	122.9(2)	122.94433	N1—C20	1.473(4)	1.47364
N1—C1—C2	116.2(2)	115.64671	N2—C10	1.354(3)	1.38096
F3—C17—C13	119.1(8)	112.11618	N2—C11	1.433(3)	1.48162
N2—C18—C19	113.6(3)	113.61563	N2—C18	1.480(3)	1.42692
Compound 11					

C1A—N1A—C9A	123.16(18)	123.44171	O1A—C1A	1.231(2)	1.22289
C1A—N1A—C17A	116.57(19)	115.74820	O2A—C10A	1.223(3)	1.21936
C9A—N1A—C17A	120.3(2)	120.77735	N1A—C1A	1.389(3)	1.40833
C10A—N2A—C11A	123.96(17)	124.28665	N1A—C9A	1.397(3)	1.39376
C10A—N2A—C20A	117.2(2)	117.06747	N1A—C17A	1.470(3)	1.47149
C11A—N2A—C20A	118.82(19)	117.63524	N2A—C10A	1.350(3)	1.37826
O1A—C1A—N1A	121.2(2)	121.44592	N2A—C11A	1.432(3)	1.43654
O1A—C1A—C2A	122.9(2)	123.24597	N2A—C20A	1.475(3)	1.47545
N1A—C1A—C2A	115.88(17)	115.30811	C1A—C2A	1.441(3)	1.45453
O2A—C10A—N2A	122.8(2)	122.61845	C2A—C3A	1.340(3)	1.35132
O2A—C10A—C3A	119.40(19)	119.86221	C3A—C4A	1.440(3)	1.44736
N2A—C10A—C3A	117.62(17)	117.46279	C3A—C10A	1.502(3)	1.51222
Compound 15					
C16—O4—C17	116.08(19)	116.51546	O1—C1	1.226(3)	1.22337
C11—O6—C12	116.8(2)	116.21487	O2—C14	1.223(2)	1.21932
C1—N1—C9	123.48(16)	123.39328	O3—C16	1.198(2)	1.20435
C1—N1—C10	116.80(17)	115.79115	O4—C16	1.325(2)	1.34175
C9—N1—C10	119.69(16)	120.80438	O4—C17	1.464(3)	1.45222
C14—N2—C15	116.79(16)	116.06128	O5—C11	1.190(3)	1.20114
C14—N2—C19	124.24(15)	124.14860	O6—C11	1.317(3)	1.34712
C19—N2—C15	117.60(15)	118.32629	O6—C12	1.459(4)	1.45120
O1—C1—N1	121.34(19)	121.17736	N1—C1	1.382(2)	1.40882
O1—C1—C2	123.13(18)	123.39068	N1—C9	1.390(3)	1.39342
N1—C1—C2	115.52(17)	115.42804	N1—C10	1.453(2)	1.45186
Compound 18					
C18—O3—C19	121.3(3)	120.91140	F1—C25	1.331(4)	1.35031
C22—O6—C23	116.02(18)	116.65320	F2—C25	1.306(4)	1.35553
C1—N1—C9	123.59(16)	123.46631	F3—C25	1.363(4)	1.34952
C1—N1—C17	116.90(17)	115.83665	O1—C1	1.230(3)	1.22326
C9—N1—C17	119.47(16)	120.69077	O2—C18	1.196(4)	1.20192
C10—N2—C11	124.32(15)	124.71138	O3—C18	1.324(3)	1.34725
O1—C1—N1	121.35(18)	121.22491	O3—C19	1.428(5)	1.45364
O1—C1—C2	123.16(18)	123.39693	O4—C10	1.218(3)	1.21714
N1—C1—C2	115.49(17)	115.37814	O5—C22	1.195(2)	1.20686
N1—C9—C4	119.80(16)	119.67303	O6—C22	1.327(2)	1.33664
N1—C9—C8	121.84(18)	121.47893	O6—C23	1.462(3)	1.45467
C8—C9—C4	118.35(19)	118.84534	N1—C1	1.380(2)	1.40895
O4—C10—N2	122.07(18)	121.40431	N1—C9	1.392(3)	1.39311

Table 3. The global reactivity descriptors calculated in the gas phase for compounds 10, 11, 15 and 18.

Parameters (eV)	Compound 10	Compound 11	Compound 15	Compound 18
E_{LUMO} (eV)	-1.9521	-1.9353	-1.7200	-1.9176
E_{HOMO} (eV)	-6.1794	-6.2747	-6.0875	-6.2148
Energy band gap $ E_{HOMO} - E_{LUMO} $	4.2273	4.3394	4.3675	4.2972
Ionization potential ($I = -E_{HOMO}$)	6.1794	6.2747	6.0875	6.2148
Electron affinity ($A = -E_{LUMO}$)	1.9521	1.9353	1.7200	1.9176
Chemical hardness ($\eta = (I-A)/2$)	2.1137	2.1697	2.1838	2.1486
Chemical softness ($\xi = 1/2\eta$)	0.2366	0.2304	0.2290	0.2327
Electronegativity ($\chi = (I+A)/2$)	4.0658	4.1050	3.9038	4.0662
Chemical potential ($\mu = -(I+A)/2$)	-4.0658	-4.1050	-3.9038	-4.0662
Electrophilicity index ($\omega = \chi^2/2\eta$)	3.9104	3.8833	3.4892	3.8476
Maximum charge transfer index ($\Delta N_{max} = -\mu/\eta$)	1.9236	1.8920	1.7876	1.8925

Table 4. The experimental and computed ^{13}C -NMR isotropic chemical shifts (with respect to TMS, all values in ppm) for compounds 10, 11, 15 and 18.							
Compound 10		Compound 11		Compound 15		Compound 18	
$\delta_{\text{exp.}}$ (Atoms)	$\delta_{\text{cal.}}$	$\delta_{\text{exp.}}$ (Atoms)	$\delta_{\text{cal.}}$	$\delta_{\text{exp.}}$ (Atoms)	$\delta_{\text{cal.}}$	$\delta_{\text{exp.}}$ (Atoms)	$\delta_{\text{cal.}}$
166.43 (C1)	165.3	166.26(C1A)	164.5	160.71(C1)	165.3	160.51 (C1)	165.2
126.65(C2)	127.2	126.91(C2A)	125.9	127.63(C2)	124.4	127.29(C2)	124.2
139.22(C3)	153.4	138.91(C3A)	154.1	141.67(C3)	155.0	139.28(C3)	154.8
116.27(C4)	125.9	118.25(C4A)	126.0	118.19(C4)	125.9	117.80(C4)	125.3
130.79(C5)	134.4	128.61(C5A)	134.7	123.01(C5)	135.9	123.12(C5)	135.8
124.70(C6)	127.5	122.95(C6A)	128.2	119.47(C6)	127.8	119.50(C6)	128.2
131.28(C7)	138.0	131.27(C7A)	138.0	131.39(C7)	137.8	131.69(C7)	138.2
114.57(C8)	119.6	115.04(C8A)	120.5	113.81(C8)	119.2	113.95(C8)	119.1
139.80(C9)	148.3	140.62(C9A)	147.7	139.29(C9)	147.9	145.06(C9)	148.0
163.05(C10)	175.1	160.06 (C10A)	174.2	167.20(C14)	175.6	167.08(C10)	175.6
145.87(C11)	155.1	145.09 (C11A)	150.0	43.79(C10)	46.5	145.87(C11)	151.3
124.17(C12)	130.0	127.45(C12A)	135.8	167.72(C11)	176.9	130.85(C12)	134.7
126.82(C13)	137.9	127.45(C13A)	135.5	61.73(C12)	68.1	125.15(C13)	138.8
119.21(C14)	130.6	119.80(C14A)	135.2	14.05(C13)	15.9	130.29(C14)	134.1
122.40(C15)	136.9	129.57(C15A)	136.5	51.53 (C15)	56.1	129.21(C15)	136.9
130.14(C16)	134.4	129.57(C16A)	134.0	61.77 (C17)	68.3	129.21(C16)	140.9
44.50(C18)	53.0	31.63(C17A)	33.8	14.21(C18)	16.0	43.81(C17)	46.7
13.04(C19)	16.5	77.51(C18A)	82.6	145.45(C19)	151.5	167.57(C18)	176.6
37.23(C20)	41.5	72.60(C19A)	75.0	129.58(C20)	136.9	61.75(C19)	67.1
12.49(C21)	13.8	38.88(C20A)	42.7	129.58(C21)	135.6	14.16(C20)	16.4
129.45(C17)	134.9	78.24(C21A)	83.1	128.42(C22)	135.5	51.35(C21)	55.8
-	-	72.89(C22A)	75.4	127.31(C23)	136.2	168.34(C22)	178.5
-	-	-	-	127.31(C24)	135.2	62.01(C23)	68.6
-	-	-	-	168.55(C26)	178.1	14.00(C24)	15.9
-	-	-	-	-	-	124.21(C25)	135.0

Table 5. The experimental and computed ¹H-NMR isotropic chemical shifts (with respect to TMS, all values in ppm) for compounds 10, 11, 15 and 18.

Compound 10		Compound 11		Compound 15		Compound 18	
δexp.(Atoms)	δcal.	δexp. (Atoms)	δcal.	δexp. (Atoms)	δcal.	δexp. (Atoms)	δcal.
6.35 (H2A)	6.06	6.42(H2A)	6.15	6.49(H2A)	6.23	6.46(H2A)	6.27
7.56-7,7 (H5A)	8.25	7.81(H5A)	8.23	7.03-8.08 (H5A)	8.38	8.00-8.03(H5A)	8.39
7.26-7.4 (H6A)	7.52	7.18-7.22(H6A)	7.57	7.03-8.08(H6A)	7.55	7.00-7.51(H6A)	7.56
7.26-7.4(H7A)	7.87	7.6(H7A)	7.89	7.03-8.08(H7A)	7.78	7.00-7.51(H7A)	7.77
7.26-7.4(H8A)	7.50	7.18-7.22(H8A)	7.58	7.03-8.08(H8A)	7.03	7.00-7.51(H8A)	7.01
7.26-7.4(H12A)	7.09	7.33(H12A)	7.64	7.03-8.08(H20A)	7.61	7.00-7.51(H16A)	7.81
7.26-7.4(H13A)	7.63	7.46(H13A)	7.73	7.03-8.08(H21A)	7.65	7.00-7.51 (H14A)	7.76
7.56-7,7(H14A)	7.79	7.18-7.22(H14A)	7.53	7.03-8.08(H22A)	7.51	7.00-7.51 (H13A)	7.76
7.56-7,7(H16A)	7.93	7.18-7.22(H15A)	7.29	7.03-8.08 (H23A)	7.29	7.00-7.51 (H12A)	8.10
4.24(H20A)	3.12	7.18-7.22(H16A)	7.16	7.03-8.08(H24A)	7.62	4.93(H17A)	4.07
4.24(H20B)	4.72	4.74(H17A)	3.95	4.16(H10A)	4.05	4.93 (H17B)	5.72
1.33(H21A)	2.04	4.74(H17B)	5.95	4.16(H10B)	5.85	4.13 (H19A)	4.92
1.33(H21B)	1.55	2.21(H19A)	1.77	4.97(H12A)	4.18	4.13(H19B)	3.93
1.33(H21C)	1.25	4.97(H20A)	3.96	4.97(H12B)	4.12	1.14 (H20A)	1.37
4.09(H18A)	4.79	4.97(H20B)	5.60	1.18 (H13A)	1.48	1.14 (H20B)	1.00
4.09(H18B)	3.59	2.36(H22A)	1.88	1.18 (H13B)	1.47	1.14 (H20C)	1.27
1.25(H19A)	1.28	-	-	1.18 (H13C)	1.25	4.61 (H21A)	3.81
1.25(H19B)	1.09	-	-	4.32(H15A)	3.90	4.61(H21A)	5.22
1.25(H19C)	1.03	-	-	4.32(H15B)	5.25	4.31 (H23A)	4.30
-	-	-	-	4.65(H17A)	4.23	4.31(H23B)	4.40
-	-	-	-	4.65(H17B)	4.35	1.32 (H24A)	1.53
-	-	-	-	1.36 (H18A)	1.28	1.32 (H24B)	1.30
-	-	-	-	1.36 (H18B)	1.42	1.32(H24C)	1.45
-	-	-	-	1.36 (H18C)	1.51	-	-

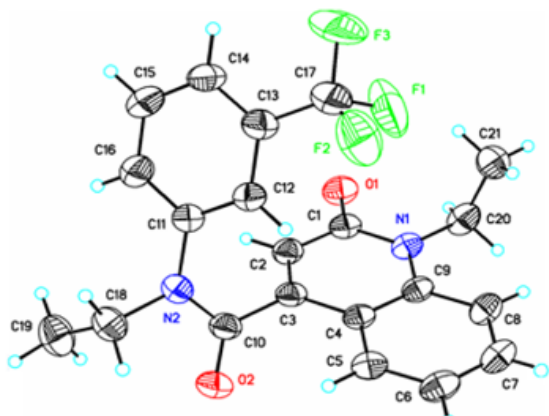
Table 6. AutoDock Vina results of the binding affinities and RMSD values for ten different poses for compounds 10, 11, 15 and 18.

Mode	for compound 10			for compound 11		
	Affinity (kcal/mol)	RMSD l.b.	RMSD u.b.	Affinity (kcal/mol)	RMSD l.b.	RMSD u.b.
1	-8.40	0.000	0.000	-8.80	0.000	0.000
2	-8.30	3.998	7.627	-8.60	0.793	2.440
3	-8.30	3.890	6.274	-8.40	1.880	2.488
4	-8.20	4.122	7.517	-8.20	2.356	5.240
5	-8.20	3.913	7.120	-8.10	1.274	6.725
6	-8.10	2.084	3.808	-7.80	2.528	6.726
7	-8.00	2.833	5.578	-7.50	2.194	6.004
8	-7.90	2.870	5.444	-7.50	2.616	3.636
9	-7.90	3.136	4.795	-7.50	2.093	2.925
10	-7.90	2.443	4.220	-7.40	2.092	6.608
	for compound 15			for compound 18		
1	-7.80	0.000	0.000	-8.60	0.000	0.000
2	-7.50	1.915	2.566	-8.40	2.768	6.314
3	-7.50	1.684	3.443	-8.40	4.532	6.458
4	-7.50	2.430	4.413	-8.40	4.569	6.971
5	-7.50	2.830	4.722	-8.40	2.124	6.756
6	-7.20	2.050	3.442	-8.10	4.165	7.344
7	-7.20	1.727	3.588	-8.00	3.935	5.807
8	-7.10	1.382	1.962	-8.00	1.935	2.439

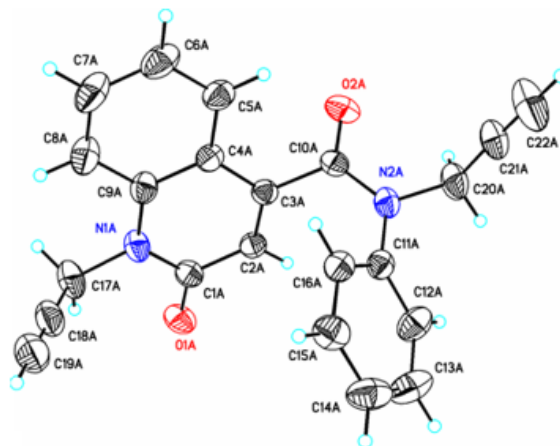
9	-7.00	1.860	6.160	-7.90	3.783	7.927
10	-6.70	2.413	4.415	-7.90	3.294	7.072

Table 7. The inter-molecular hydrogen bond interactions and their distances *between compounds 10, 11, 15 and 18 with the macromolecule 1M17.*

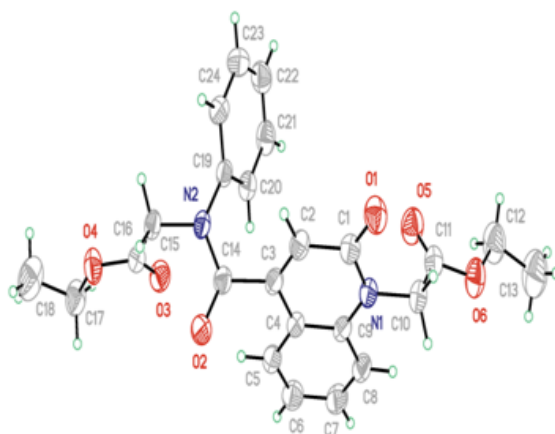
for the compound 10			
Residue group	Ligand group	Distance (Å)	Interaction
OH group in THR830	=O atom in carboxamide	3.18	Conventional hydrogen bond
CH ₂ group in GLY772	F atom in trifluoromethyl	3.34	Carbon hydrogen bond
for the compound 11			
Residue group	Ligand group	Distance (Å)	Interaction
OH group in THR830	=O atom in in oxoquinolin	2.90	Conventional hydrogen bond
for the compound 15			
Residue group	Ligand group	Distance (Å)	Interaction
NH ₂ group in LYS721	=O atom in oxoquinolin	3.14	Conventional hydrogen bond
OH group in THR766	O atom in ethyl acetate	2.98	Conventional hydrogen bond
OH group in THR830	=O atom in ethyl acetate	2.97	Conventional hydrogen bond
Sg group in CYS751	=O atom in ethyl acetate	3.37	Conventional hydrogen bond
for the compound 18			
Residue group	Ligand group	Distance (Å)	Interaction
OH group in THR766	O atom in ethyl acetate	3.00	Conventional hydrogen bond
OH group in THR830	=O atom in ethyl acetate	2.79	Conventional hydrogen bond



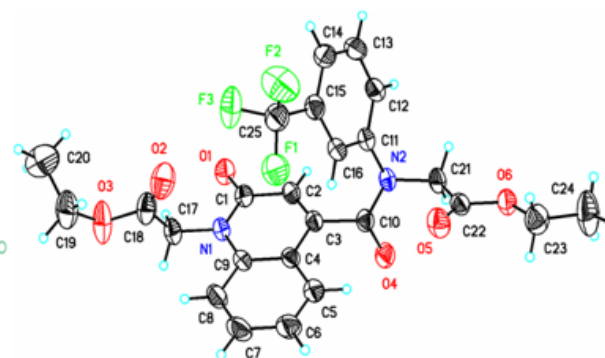
Compound 10



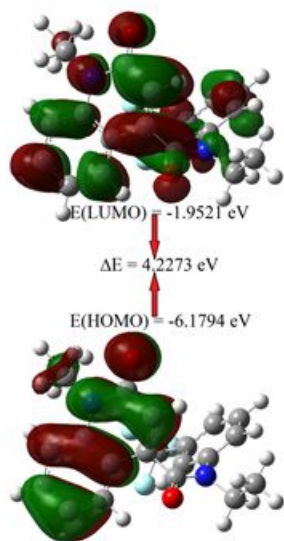
Compound 11



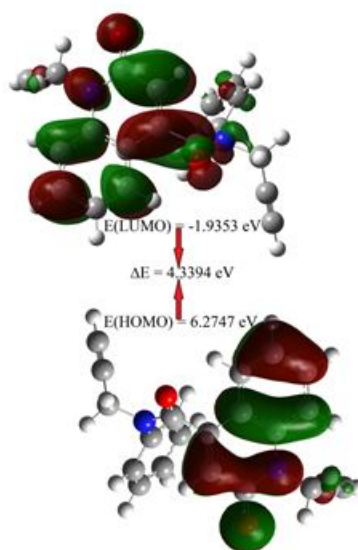
Compound 15



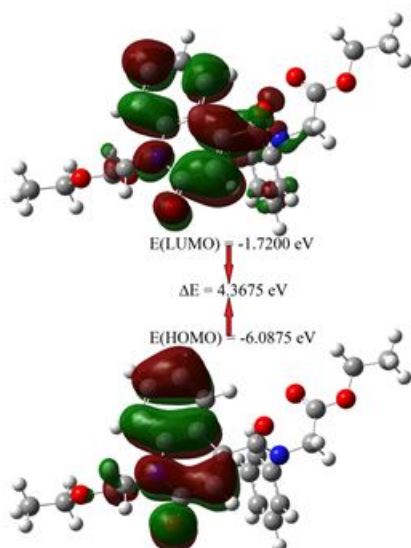
Compound 18



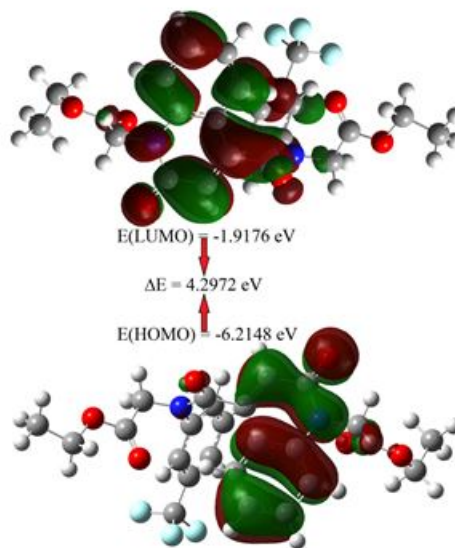
Compound 10



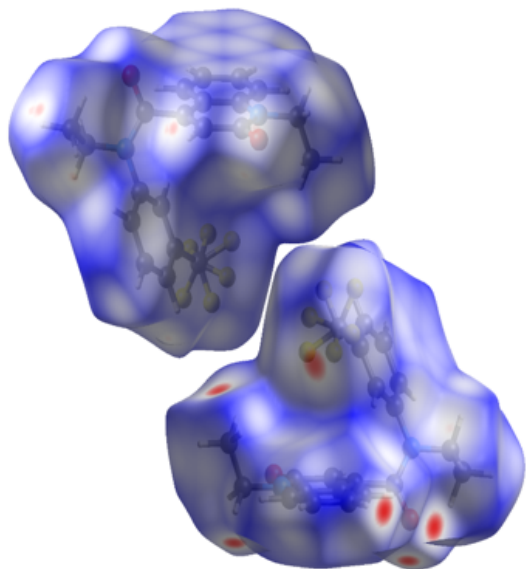
Compound 11



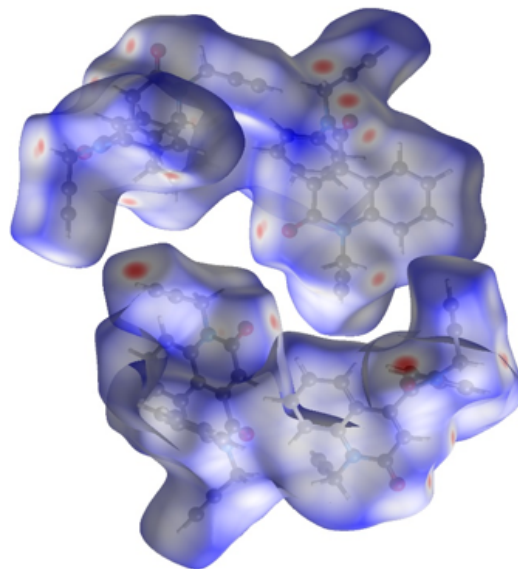
Compound 15



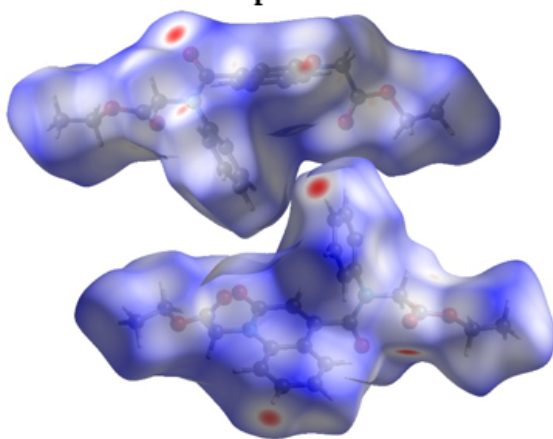
Compound 18



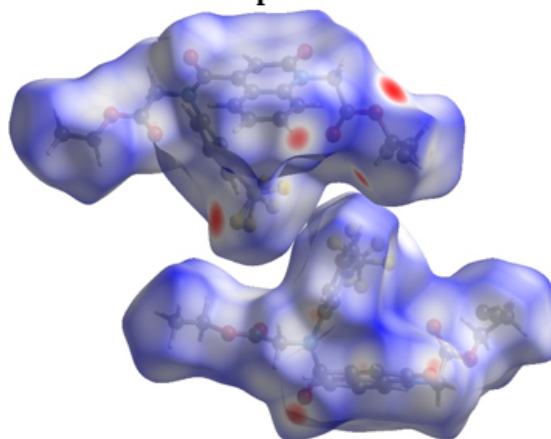
Compound 10



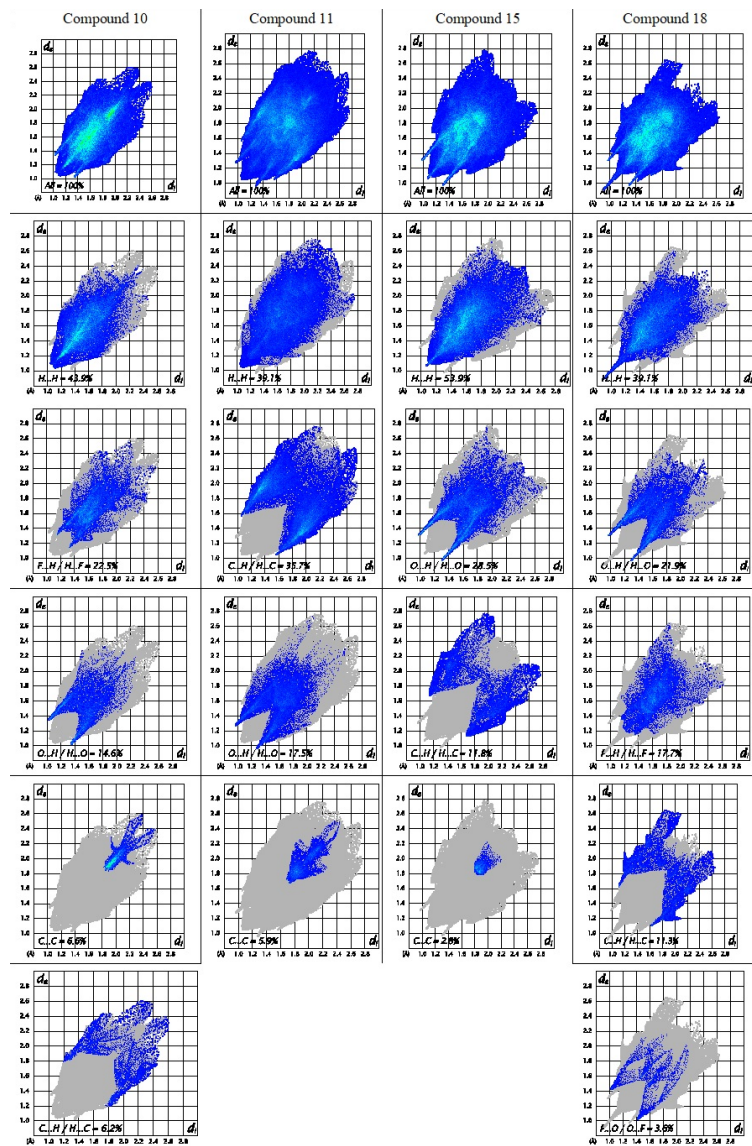
Compound 11



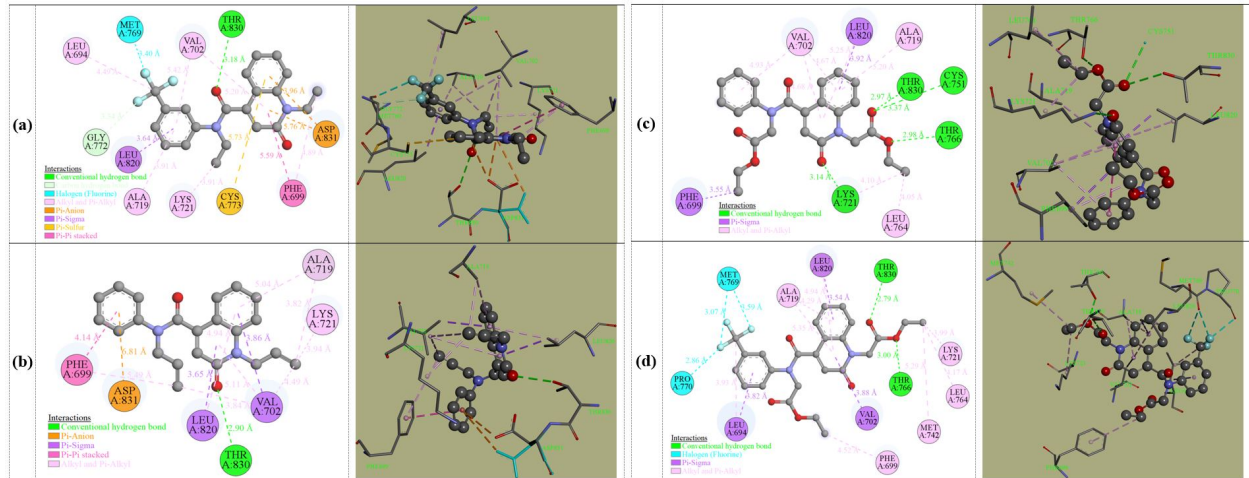
Compound 15



Compound 18



PROOF



Journal Pre-proof

Highlights

- Synthesis of new N-substituted 2-oxo-1,2-dihydroquinoline carboxamide derivatives.
- 3D molecular structure is characterized using X-ray and spectroscopic techniques.
- Good correlations are obtained between the spectra and X-ray data with the predicted ones.
- Hirshfeld surface analysis was used to analyze the intermolecular interaction.
- Molecular docking studies, and DFT calculations.

Syntheses of novel 2-oxo-1,2-dihydroquinoline derivatives: molecular and crystal structures, spectroscopic characterizations, Hirshfeld surface analyses, molecular docking studies and Density Functional Theory calculations.

Yassir Filali Baba^a, Halil Gökce^b, Youssef Kandri Rodi^a, Sonia Hayani^a, Fouad Ouazzani Chahdi^a, Abdellatif Boukir^c, Jerry P. Jasinski^d, Manpreet Kaur^d, Tuncer Hökelek^e, Nada Kheira Sebbar^{f,g*}, El Mokhtar Essassi^f

^aLaboratory of Applied Organic Chemistry, Faculty of Science and Techniques, Sidi Mohamed Ben Abdellah University, B.P. 2202, Routed 'Imouzzar, Fez 30050, Morocco;

^bGiresun University, Vocational High School of Health Services, Department of Medical Services and Techniques, 28100 Giresun, Turkey;

^cLaboratory of Biotechnology Microbien and Molecules Bioactives LB2MB, Faculty of Science and Techniques, Sidi Mohamed Ben Abdellah University, B.P. 2202, Route 'Imouzzar, Fez 30050, Morocco;

^dDepartment of Chemistry, Keene State College, 229 Main Street, Keene, NH 03435-2001, USA;

^eDepartment of Physics, Hacettepe University, 06800 Beytepe, Ankara, Turkey;

^fLaboratoire de Chimie Appliquée et Environnement, Equipe de Chimie Bioorganique Appliquée, Faculté des sciences, Université Ibn Zohr, Agadir, Morocco;

^gLaboratoire de Chimie Organique Hétérocyclique, Centre de Recherche des Sciences des Médicaments, Pôle de Compétences Pharmacochimie, Mohammed V University in Rabat, Faculté des Sciences, Av. Ibn Battouta, BP 1014 Rabat, Morocco.

Credit Author Statement

The work presented here was carried out in collaboration between all authors. **Youssef Kandri Rodi, Halil Gökce, Sonia Hayani, Fouad Ouazzani Chahdi, Abdellatif Boukir, Nada Kheira Sebbar** and **El Mokhtar Essassi** defined the research theme. **Yassir Filali Baba, Sonia Hayani** and **Youssef Kandri Rodi** carried out the Syntheses of novel 2-oxo-1,2-dihydroquinoline derivatives: molecular and crystal structures, spectroscopic characterizations, Hirshfeld surface analyses, molecular docking studies and Density Functional Theory calculations. **Yassir Filali Baba**, wrote the paper with **Youssef Kandri Rodi, Halil Gökce, Tuncer Hökelek, Nada Kheira Sebbar** and **El Mokhtar Essassi**.

Halil Gökce, Performed the analysis Gaussian 09 calculations and Especially theoretical spectroscopy sections and molecular docking and interpretation. Discussed, interpreted, and presented the data.

Jerry P. Jasinski and **Manpreet Kaur** co-worked on Collected the data DRX data and interpretation. Discussed, interpreted, and presented the data.

All authors read and approved the final manuscript.

Disclosure statement

No potential conflict of interest was reported by the authors.

Journal Pre-proof